Article

Not peer-reviewed version

Dynamic Model for Risk Assessment and Prevention of Road Traffic Accidents Involving Pedestrians

Hristo Uzunov , Plamen Matzinski , Vasil Uzunov , Silvia Dechkova *

Posted Date: 17 March 2026

doi: 10.20944/preprints202603.1262.v1

Keywords: road traffic accidents; pedestrians; risk assessment; driver reaction time; dynamic modelling; traffic safety

Article

Dynamic Model for Risk Assessment and Prevention of Road Traffic Accidents Involving Pedestrians

Hristo Uzunov, Plamen Matzinski, Vasil Uzunov and Silvia Dechkova *

Faculty of Engineering and Pedagogy, Technical University of Sofia, 1000 Sofia, Bulgaria

* Correspondence: sdechkova@tu-sofia.bg; Tel.: +359-8-97022422

Featured Application

The proposed model can be applied in intelligent transportation systems, driver assistance technologies, and forensic accident analysis to evaluate pedestrian-related traffic risks and support the development of automated collision prevention systems.

Abstract

Pedestrian-involved road traffic accidents represent a serious challenge for traffic safety and require a comprehensive analysis of the interactions within the driver–vehicle–road–environment system. The objective of this study is to develop a methodology for risk assessment in road traffic accidents involving pedestrians based on the analysis of real court cases and dynamic modeling of vehicle motion. A database of 105 court cases was analyzed, enabling the identification of the main factors influencing the occurrence of pedestrian-related accidents. Based on this analysis, a system of 31 linguistic variables was developed to characterize driver behavior, vehicle technical characteristics, and road environment conditions. These variables were integrated into a mathematical model for quantitative risk assessment that enables the evaluation of the relative influence of different groups of factors on accident probability. In addition, a dynamic model of vehicle motion was developed to analyze the influence of driver reaction time, vehicle speed, and road surface conditions on the possibility of avoiding a collision. The results of the numerical analysis demonstrate that even minimal delays in hazard perception and driver reaction significantly increase the probability of pedestrian-related accidents. These findings highlight the importance of early hazard detection and automated emergency braking systems. The proposed methodology provides a framework for integrating intelligent driver assistance systems and automated braking control aimed at improving the safety of vulnerable road users.

Keywords: road traffic accidents; pedestrians; risk assessment; driver reaction time; dynamic modelling; traffic safety

---

1. Introduction

Pedestrian-involved road traffic accidents represent a significant challenge for traffic safety and require a comprehensive and multifactorial analysis of the driver–vehicle–road–environment system. With the increasing level of urbanization and traffic intensity, pedestrians remain among the most vulnerable road users in the transport system, and the consequences of such incidents are often severe or fatal. In this context, contemporary research indicates the need not only for descriptive studies but also for an in-depth analysis of the dynamic interactions within the driver–vehicle–road–environment system. Such an analysis should consider both the human factor and the potential for automated risk assessment and management through intelligent warning and emergency braking systems.

The analysis of data from judicial practice related to road traffic accidents involving pedestrians shows that such events do not arise from a single isolated factor but rather from the accumulation

 doi:10.20944/preprints202603.1262.v1

and complex interaction between human behavior, vehicle characteristics, infrastructure and variable environmental conditions. The examined court decisions clearly indicate that the combination of factors such as instantaneous vehicle speed, driver reaction time, visibility conditions and road environment characteristics creates critical scenarios in which even minimal delays or deviations from expected behavior may lead to accidents with severe consequences. In this context, the model proposed by Elvik [1] demonstrates that even a small change in speed leads to a disproportionate increase in accident risk. Judicial practice also confirms that in many cases the combination of changes in pedestrian movement behavior, reduced friction between the tires and the road surface, and driver distraction results in a rapid increase in risk [2,3]. Similar conclusions are supported by studies examining accident data associated with behavioral heterogeneity and age differences among drivers [4]. These observations highlight the importance of dynamic modelling of interactions within the driver–vehicle–road–environment system for quantitative risk assessment.

The causes of accident occurrence should be considered within the context of the specific situational conditions at a given moment. This situation is characterized by the physical parameters of the environment, the condition of drivers and pedestrians, and their ability to adequately assess risk and make timely decisions. Judicial practice indicates that the interaction between these factors determines the critical development of events, for example a delay in the driver's perception of danger combined with unexpected pedestrian behavior, particularly under unfavorable road surface conditions. Available data indicate that the specific actions of the pedestrian at the moment of the accident are decisive for the severity of the resulting injuries [5], while detailed diagnostic analyses emphasize the significant influence of environmental conditions such as lighting, visibility, and road surface condition on the final outcome of road traffic accidents [6].

Special attention should also be given to the importance of research on dynamic risk management using modern technologies and analytical tools. Advanced methods based on machine learning, probabilistic models and real time simulations [7] provide the possibility to predict hazardous situations before they occur and to make decisions within extremely short time intervals measured in milliseconds, which are practically unattainable for human reaction. Therefore, approaches based on hazard prediction algorithms known as Time to Collision (TTC) [8] enable adaptive and progressive decision making through which the possibility of collision can be significantly reduced. Improved TTC algorithms [9] further increase prediction accuracy in different scenarios involving static, moving and accelerating objects and form the basis for more realistic risk management models. All these developments demonstrate that the integration of analytical algorithms and automated systems represents an effective approach for reducing the risk of road traffic accidents involving pedestrians. Empirical studies conducted under real conditions [10] confirm that automated emergency braking (AEB) and forward collision warning (FCW) systems reduce the frequency of pedestrian-related accidents by 25–30%, and even more when used in combination [11].

In the dynamic assessment of risk and the identification of causes leading to road traffic accidents involving pedestrians, the implementation of modern vehicle systems plays a key role by extending human capabilities and reducing the critical interval between the emergence of danger and the initiation of preventive actions. The time between the appearance of a hazard and the occurrence of a collision is largely determined by the driver reaction time, which under real conditions varies within a wide range from approximately 0.8 s in expected situations to more than 2.5 s in sudden and unpredictable events. This parameter is decisive for the possibility of accident prevention. In other words, when the perception of danger occurs in time or even before its actual realization, the probability of successfully preventing a collision becomes significantly higher. Consequently, minimizing hazard detection time and reaction time is a critical factor for improving safety, and this is precisely where automated systems demonstrate a substantial advantage by eliminating delays inherent to human perception and motor response.

Zhang et al. [12,13] have extensively analyzed the factors influencing driver reaction time. The presented research emphasizes the need for the development and integration of models capable of

 doi:10.20944/preprints202603.1262.v1

automatically assessing risk and initiating appropriate actions without relying on the human factor. Scientific studies conducted under real road conditions are also of considerable importance [14]. Their analysis indicates that each event is characterized by a number of parameters, providing a basis for conclusions regarding their influence on driver reaction time. Similar studies have shown that age has only a minor influence on the reaction time of professional heavy vehicle drivers [15]. The obtained results demonstrate the significant influence of parameters describing a given event on the delay between hazard occurrence and hazard perception.

Modern trends in automotive engineering are focused on the development of intelligent transport systems whose ultimate goal is the creation of fully autonomous vehicles. Achieving this level of autonomy is based on integrated dynamic models and artificial intelligence that perform real time environmental assessment, identify hazardous situations and make decisions without the need for human intervention. Sensor technologies such as radar, LiDAR, and cameras play a fundamental role in this process by detecting objects in the vehicle surroundings, recognizing them, and predicting their trajectories. Based on this information, the system automatically initiates preventive actions, including the activation of braking torque, in order to avoid collisions.

Warning and autonomous driver assistance systems play a key role in improving safety and preventing such collisions. The outputs of these systems involve decision making either by issuing visual and acoustic warnings to the driver through Forward Collision Warning (FCW) systems or by activating automated braking through Autonomous Emergency Braking (AEB) systems. The effectiveness of FCW and AEB systems has been confirmed in numerous studies. It has been established that FCW reduces the risk of rear end collisions by up to 27 percent, while AEB at low speeds can reduce such crashes by up to 43%. When used in combination, these systems may reduce such accidents by up to 50 percent [16]. In pickup trucks, FCW and AEB systems also demonstrate considerable effectiveness, with reductions of rear end crashes by 22 percent and 34 percent respectively [17]. Additional evaluations of Advanced Driver Assistance Systems (ADAS) technologies indicate that their large scale implementation could prevent up to 8700 crashes and approximately 70 fatalities annually [18]. Systematic reviews and real world tests using dashcam recordings also confirm their positive impact on road safety [19,20].

Additional analyses have been conducted on braking distances and maneuvers of different types of vehicles, including bicycles and other light vehicles [21], as well as on motion parameters during overtaking on two-lane roads investigated through driving simulator experiments under realistic conditions [22].

These systems significantly reduce the time interval between the occurrence of danger and the initiation of appropriate actions, achieving response times of only a few tens of milliseconds, which are practically unattainable for humans. In this way, the technological response precedes human reaction time and significantly increases the probability of avoiding or mitigating the consequences of an accident.

The integrated approach includes probabilistic risk analysis in real time, kinematic modeling of the vehicle and surrounding objects, simulation of different behavioral scenarios of pedestrians and drivers, and decision making systems based on priority and urgency. The need for such technologies is particularly evident in urban areas, where pedestrians often enter the roadway without fully recognizing the potential danger and consequently fall within the vehicle stopping distance zone. In such situations, the possibility of preventing an accident depends on the accurate and timely identification of hazard occurrence, a task that often exceeds the capabilities of the driver. For this reason, the implementation of modern risk assessment models and active automated intervention should not be considered merely a technological advancement but rather a fundamental and necessary step toward reducing road traffic injuries and creating a safer transport environment.

In this context, the present research is aimed at developing a clearly defined methodology and a dynamic model of the interaction within the elements of the transport system driver–vehicle–road–environment and pedestrian behavior. The main objective of the study is to develop a dynamic model for quantitative risk assessment in vehicle–pedestrian interactions that combines the analysis of real

 doi:10.20944/preprints202603.1262.v1

court cases, a system of linguistic variables and kinematic modeling of the motion of the involved participants. Through such an integrated system, delays associated with human reaction time can be eliminated, thereby enabling a scientifically grounded approach for minimizing risk in critical traffic situations.

The scientific contribution of this research lies in the development of an integrated model for risk assessment in road traffic accidents involving pedestrians that combines the analysis of court cases, linguistic variables and dynamic modeling of the interaction between the vehicle and the pedestrian. Based on this framework, a methodology for quantitative risk assessment and simulation of critical traffic situations has been developed, which is presented in the following section.

2. Methods

The proposed methodology is based on an integrated systems approach that combines the analysis of real court cases, experimental determination of driver reaction time and mathematical modeling of the dynamic interaction between a vehicle and a pedestrian within the driver–vehicle–road–environment transport system.

The developed methodology for risk assessment in road traffic accidents involving pedestrians serves as a basis for the creation of a dynamic model describing the behavior of the vehicle and the pedestrian under real traffic conditions. Within this model, a system for risk analysis and quantitative risk evaluation is constructed, as well as a mechanism for automated control of braking torque depending on the moment of hazard occurrence In contrast to the approaches discussed in the literature review, which are often limited either to experimental studies of driver reaction time [10–13] or to risk prediction algorithms based on generalized Time-to-Collision (TTC) models [7–9], the present methodology incorporates empirical data derived from judicial practice and linguistic variables extracted from multiple real cases with fatal outcomes. This feature enables more realistic modeling of the interaction between the elements of the driver–vehicle–road–environment system and the pedestrian as a participant in traffic. The proposed approach creates a foundation for automated decision-making in real time and extends the applicability of existing research both in forensic traffic accident reconstruction and in engineering analyses of transport safety.

To evaluate the interaction between the elements of the system, each road traffic accident of this type can be divided into three main phases. The first phase includes the period from hazard occurrence to the moment of impact. The second phase represents the collision process itself. The third phase describes the motion of the involved bodies after the impact until their final stop.

Figure 1 illustrates the transport system describing the interaction between the driver, the vehicle, the road, and the surrounding environment, where the pedestrian acts as a disturbance element. Each situation should be considered as an interaction between the elements of the system driver, vehicle and road with environment, as well as the time–spatial relationship between the vehicle and the pedestrian under the given road and meteorological conditions.

An analysis was performed on 105 real cases from judicial practice in the Republic of Bulgaria, where court decisions with either conviction or acquittal were issued in road traffic accidents involving pedestrians. The results of the analysis show that a significant systemic problem in the examined transport configuration is the discrepancy between the moment of hazard occurrence from the pedestrian's side and the moment when this hazard is perceived by the driver. In many cases the identified delay in perception reaches approximately 1.8–2 s, which corresponds to the upper limit of human reaction time. In other words, the distance travelled before the impact may nearly double before the initiation of emergency braking.

 doi:10.20944/preprints202603.1262.v1

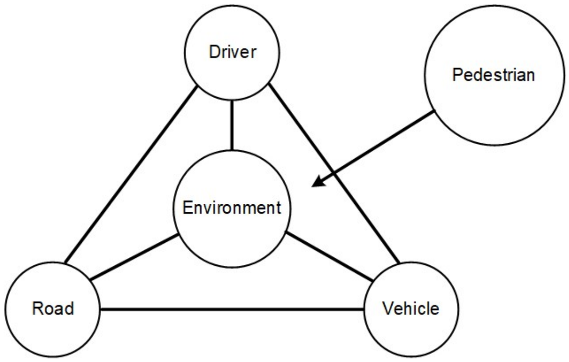

Figure 1. Schematic representation of the driver–vehicle–road–environment transport system with pedestrian involvement.

Any delay in initiating a reaction leads to a significant increase in accident risk. This delay is a dynamic variable influenced by numerous factors such as the physical and psychological condition of the driver (fatigue or stress), visibility conditions, meteorological factors and distracting elements in the surrounding environment. These behavioral scenarios associated with delayed reactions are among the most frequently observed and are directly related to the human factor.

These findings highlight the necessity of developing and implementing automated systems for risk assessment and management that compensate for human reaction delays through early hazard detection and the timely initiation of actions aimed at avoiding or mitigating the consequences of a collision.

In the developed dynamic model simulating the interaction between a vehicle and a pedestrian, an integrated system for risk analysis and assessment has been implemented, as well as a mechanism for controlling braking torque depending on the moment when the hazard occurs. Through this system, the probability of a road traffic accident involving a pedestrian is reduced and the effectiveness of preventive actions is improved.

The functional objective of the developed system is to compensate for the delay in perception and reaction that is inherent to the human factor when a hazard arises. Through continuous monitoring and analysis of the surrounding environment, the model enables identification of potential threats at an early stage and activates appropriate warning or automated actions without the need for human intervention. This significantly reduces driver reaction time and considerably lowers the risk of a collision while ensuring higher system reliability and efficiency through timely activation of braking torque. As a result, a higher level of safety is achieved both for pedestrians and for other road users.

Through detailed examination of court decisions and their underlying reasoning, as well as a systematic analysis of the factors contributing to accident occurrence, the leading role of the human factor in risk assessment and safety within the transport system has been confirmed. The analysis of interactions within the driver–vehicle–road system reveals significant differences in the relative influence of the individual components.

Based on the analysis of 105 court decisions from different judicial regions of the Republic of Bulgaria related to severe road traffic accidents involving pedestrians, 31 linguistic variables were identified. These variables represent measurable or qualitative characteristics of the different components of the transport system that influence the risk of accident occurrence. Each identified variable is associated with a set of terms classified in ascending order according to the level of risk. This enables a quantitative evaluation of the factors affecting road safety. Risk assessments for The terms are expressed as percentage values ranging from 10% to 90%, with the evaluation based on expert analysis and systematic processing of the judicial data.

The weights of the individual terms were determined through expert evaluation based on a comparative analysis of the examined court cases, taking into account both the frequency of occurrence of the respective factors and their influence on the occurrence of road traffic accidents.

Preprints.org (www.preprints.org) | NOT PEER-REVIEWED | Posted: 17 March 2026 doi:10.20944/preprints202603.1262.v1

The structure of the transport system and the relationships between its components are visualized through a diagram (Figure 2), which illustrates the influence of the linguistic variables on risk. These variables provide the basis for performing quantitative assessments of the risk of severe road traffic accidents involving pedestrians.

The "Driver" component is defined by 15 linguistic variables, indicated in the diagram as follows:

1.1 Current speed
1.2 Maneuver
1.3 Use of alcohol or narcotic substances by the driver
1.4 Driver experience
1.5 Occurrence of hazard
1.6 Pedestrian behavior
1.7 Perception of hazard
1.8 Initiated braking
1.9 Pedestrian age
1.10 Direction of movement
1.11 Use of alcohol or narcotic substances by the pedestrian
1.12 Comparability of distances at the current speed
1.13 The stopping distance at the current speed is shorter than the distance to the point of impact
1.14 Comparability of distances at the regulated speed
1.15 The stopping distance at the regulated speed is shorter than the distance to the point of impact.

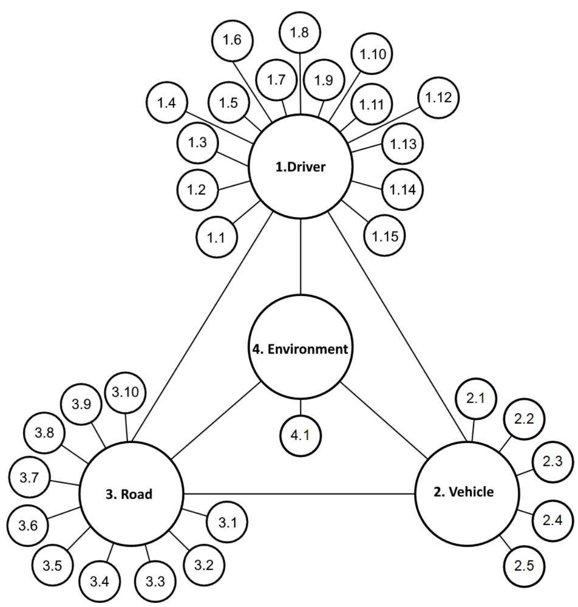

Figure 2. Structural diagram of the driver–vehicle–road–environment transport system.

It was established that driver behavior and condition have the most significant influence on the occurrence of road traffic accidents, while the contribution of vehicle technical condition and road infrastructure characteristics is less pronounced. According to Abdel-Aty et al. [23], human behavior remains the leading factor in risk modeling, as even modern machine learning algorithms identify it as a primary cause of road traffic accidents.

The vehicle component is defined by five linguistic variables indicated in the diagram as follows:

 doi:10.20944/preprints202603.1262.v1

2.1. Type of vehicle

2.2 Safety systems
2.3 Lighting control system
2.4 Lighting system type
2.5 Technical condition

These linguistic variables reflect the technical and functional characteristics of the vehicle that influence its behavior within the transport system.

The road component is defined by ten linguistic variables as follows:

3.1 Road surface condition
3.2 Type of road pavement
3.3 Traffic conditions
3.4 Road profile geometry
3.5 Location of the accident
3.6 Roadway width
3.7 Road conditions
3.8 Lighting conditions
3.9 Traffic regulation
3.10 Road class

The component "environment" is defined by a single linguistic variable weather conditions, which includes the following terms:

4.1 Clear weather
4.2 Cloudy weather
4.3 Rain
4.4 Fog with visibility greater than 200 m
4.5 Fog with visibility from 150 m to 199 m
4.6 Fog with visibility 100–149 m
4.7 Fog with visibility 50–99 m
4.8 Fog with visibility ≤ 49 m
4.9 Snowfall
4.10 Heavy rain
4.11 Strong wind
4.12 Hail

The total number of possible combinations between the terms of the linguistic variables is determined by the following relationship:

$$N = \prod_{i=1}^{k} n_i \tag{1}$$

The obtained relationship shows that the total number of possible system combinations is determined as the product of the number of terms of each linguistic variable, which makes it possible to account for the full set of possible states of the transport system.

where

N is the total number of possible combinations;

k is the total number of linguistic variables;

n_i is the number of terms of the i- th linguistic variable.

The output variable of the model represents the integrated risk assessment of road traffic accidents and is calculated based on weighting coefficients and the membership degrees of the linguistic variables.

 doi:10.20944/preprints202603.1262.v1

2.1. Risk Analysis Methodology

A court decision represents an official legal document that summarizes the factual circumstances of a case and provides the legal assessment of the court within a specific criminal proceeding. Its structure is regulated in order to ensure a clear and logically organized presentation of the facts and circumstances related to a particular incident.

The accusatory section contains a concise description of the charges and formulates the main issue that the court must resolve. In this section the legal qualification of the offence is presented in accordance with the applicable legal provisions.

The factual background describes the facts established during the judicial process. The chronology of events and their context serve as the basis for the court's analysis. The presented evidence, including witness testimonies, documents, and expert reports, is evaluated with respect to its reliability and relevance to the case. It should be noted that not all data included in a court decision are quantitatively measurable. Therefore, expert technical analysis is required in order to identify the factors that can be quantified, which allows a more accurate assessment of the risk associated with pedestrian related road traffic accidents.

Linguistic variables are introduced in order to systematize and formalize the factors influencing the risk of road traffic accidents involving pedestrians. They include 31 significant characteristics of the transport system and allow a more accurate and objective assessment of the conditions under which critical traffic situations arise. Each term defined within these variables describes a specific state or characteristic classified according to its severity with respect to the risk of occurrence of the considered type of road traffic accident.

Through this approach the qualitative characteristics of the analyzed traffic scenarios are represented, derived from court decisions and expert evaluation. Each variable describes a specific characteristic of the environment or the behavior of the traffic participants. For example, within the parameter visibility, the terms low, medium, and high are used. These values are formalized through a set of terms expressing the different states of the variable. Such formalization is typical of methodologies based on fuzzy set theory, in which expert knowledge is transformed into a formalized model that enables subsequent quantitative analysis.

Within the context of the present study, the use of such variables allows the systematization of factors identified in judicial practice and their incorporation into a dynamic model for risk assessment and risk management.

The combinations between the individual terms form a vector of 31 elements, which serves as the basis for the quantitative analysis of risk. These variables are grouped into three main categories of factors.

Factors related to driver behavior include 15 variables.

Factors related to the vehicle include 5 variables.

Factors related to the road environment and surrounding conditions include 11 variables.

This grouping enables evaluation of the individual contribution of each factor and the analysis of the combined influence of the different subsystems on the overall risk level within the transport system.

2.2. Mathematical Relationships for Calculating Shares and Total Contribution

2.2.1. Parameters

The proposed methodology is based on the principle of proportional distribution of the overall risk associated with pedestrian related road traffic accidents among the factors that influence its occurrence. The total risk corresponding to the analyzed type of incident is normalized to 100% and proportionally distributed among three main groups of factors: road and environmental conditions T_1, vehicle related factors T_2, and driver related factorsT_3. This normalization allows the contributions of the individual subsystems to be evaluated within a unified quantitative framework and enables a direct comparison of their relative influence on the overall level of risk.

doi:10.20944/preprints202603.1262.v1

$$T_1 + T_2 + T_3 = 100\% \tag{2}$$

The first group includes the road and environment elements, the total number of terms is 11. The second group, representing the vehicle component, contains 5 terms, while the third group, representing the driver component, contains 15 terms. The differences in the range of values arises from the different number of terms within each group.

This approach provides an objective framework for the quantitative assessment of the relative contribution of risk associated with the individual elements of the transport system. The input data used in the proposed methodology are represented by a vector of values corresponding to the 31 linguistic variables. This vector describes a specific pedestrian related road traffic accident scenario.

$$\Omega_j = [\omega_1, \omega_2, \dots, \omega_{31}] \tag{3}$$

where $\omega_1, \omega_2, \dots \dots, \omega_{31}$ are numerical values representing the relative weight associated with each term.

The weighted value of risk for each linguistic variable, relative to the total weight of group T_k, $k = 1,2,3$, is determined by the following expression:

$$S_{i,k} = \frac{\omega_{i,k}}{\sum \omega_{i,max,k}} . T_k . 100 \tag{4}$$

where:

$S_{i,k}$ is the weighted value of risk for the i-th term in group k, $i = 1,2 \dots 31$;

$\omega_{i,k}$ are numerical values characterizing the relative share of the weight assigned to each term within group k;

$\sum \omega_{i,max,k}$ is the sum of the maximum quantitative evaluations of the weights of the terms from all linguistic variables within the respective group k;

T_k represents the distribution of the total weight assigned to group k;

The distribution of weights T_k for each group k is determined as follows:

$$T_1 = \frac{\sum_{i=1}^{11} \omega_{i,1}}{\sum_{i=1}^{31} \omega_i}, \qquad T_2 = \frac{\sum_{i=12}^{16} \omega_{i,2}}{\sum_{i=1}^{31} \omega_i}, \quad T_3 = \frac{\sum_{i=17}^{31} \omega_{i,3}}{\sum_{i=1}^{31} \omega_i} \tag{5}$$

where

ω_i are numerical values characterizing the relative weight of each term from the vector Ω_j describing the analyzed scenario.

The weights of the individual factors were determined through expert evaluation based on a comparative analysis of the examined court cases. The assessment considers both the frequency of occurrence of the respective factors and their influence on the occurrence of the road traffic accident. Each variable is normalized with respect to the maximum possible value within the corresponding group of factors. This normalization ensures comparability between the individual components of the model and allows the integration of parameters of different nature into a unified quantitative risk assessment.

The total value of the risk weight is obtained as the sum of the weighted risk values for each group and is expressed as follows:

$$R_j = \sum_{i=1}^{11} S_{i,1} + \sum_{i=12}^{16} S_{i,2} + \sum_{i=17}^{31} S_{i,3} \tag{6}$$

The integrated risk index R_j represents a normalized value that summarizes the influence of all factors within the transport system. It is determined as the sum of the weighted risk values for the individual groups of factors related to the road and environmental conditions, the characteristics of the vehicle, and the behavior of the driver. In this way, the index reflects the combined influence of the components of the driver–vehicle–road–environment system on the occurrence of a road traffic accident involving a pedestrian.

 doi:10.20944/preprints202603.1262.v1

It should be emphasized that the obtained index does not represent a statistical probability of the occurrence of a road traffic accident in the strict statistical sense, but rather an integral risk assessment. The index combines the influence of the probabilistic preconditions for the occurrence of the incident, the severity of the individual factors, and their proportional contribution within the overall dynamic configuration of the transport system.

The expert evaluation derived from the analysis of real court cases determines the weight of each term within every variable and serves as the basis for constructing a proportionally weighted model. The resulting vector of 31 variables is normalized with respect to the maximum possible combination of terms, as a result of which the assessment is expressed within the interval from 0 to 100 percent.

The index defined in this way reflects an integrated level of systemic risk that includes both the probabilistic components of the incident and the severity of the conditions identified through judicial practice in Bulgaria. In this manner the resulting assessment characterizes not only the probability of occurrence but also the structural contribution of all factors in the specific momentary situation. This enables the use of the index both for the analysis of court cases and for automated decision making within dynamic models.

The proposed method for risk calculation is based on integral indices widely used in road safety research, where risk is modelled through the combination of quantitative and qualitative factors. The validity of the model is supported by empirical data obtained from the analysis of 105 real court cases, which allow calibration of the weighting coefficients of the linguistic variables. The structure of the linguistic variables and their proportional weighting correspond to approaches widely applied in fuzzy risk methodologies and expert systems.

2.3. Dynamic Model of Vehicle and Pedestrian Motion and Their Relative Coordinate System

The emergence of a hazardous situation results from pedestrian movement, assuming that the pedestrian moves in two consecutive motion phases. In the general case, the equations describing pedestrian motion over time are formulated through kinematic relationships that account for the coordinates of the center of mass, the angular rotation relative to the initial position, the velocities and accelerations of the center of mass, as well as the angular velocities and angular accelerations.

Each equation consists of two time intervals. During the first interval the motion is described by the initial velocity and acceleration, while during the second interval the final velocity of the center of mass is taken into account. The sum of these two components determines the total displacement or rotation of the pedestrian from the moment the hazardous situation arises until the pedestrian reaches the boundary of the vehicle movement corridor.

These relationships make it possible to predict the future position of the pedestrian.

$$\begin{aligned} x_{p1}(t_{p1}) + x_{p2}(t_{p2}) &= \ddot{x}_{p1}.\frac{t_{p1}^2}{2} + \dot{x}_o.t_{p1} + \dot{x}_2.t_{p2} \\ y_{p1}(t_{p1}) + y_{p2}(t_{p2}) &= \ddot{y}_{p1}.\frac{t_{p1}^2}{2} + \dot{y}_o.t_{p1} + \dot{y}_2.t_{p2} \\ \varphi_{p1}(t_{p1}) + \varphi_{p2}(t_{p2}) &= \ddot{\varphi}_{p1}.\frac{t_{p1}^2}{2} + \dot{\varphi}_o.t_{p1} + \dot{\varphi}_2.t_{p2} \end{aligned} \tag{7}$$

where

x_{p1}, x_{p2} represent the projections of the displacement of the pedestrian's center of mass along the x axis, measured from the position of the pedestrian at the moment when the hazardous situation arises to the coordinates of the point of entry into the vehicle movement corridor within two consecutive time intervals;

$\dot{x}_o, \dot{y}_o$ represent the projections of the initial velocity of the pedestrian's center of mass along the corresponding coordinate axes x and y at the moment when the hazardous situation occurs. These components determine the initial direction and intensity of pedestrian motion with respect to the global coordinate system;

 doi:10.20944/preprints202603.1262.v1

$\ddot{x}_p$, $\ddot{y}_p$ represent the projections of the average acceleration of the pedestrian's center of mass along the corresponding axes x and y within the considered time interval. They reflect the change in the velocity of the centre of mass in the direction of motion and are used to determine the nonlinear component of the travelled distance;

t_{p1} represents the time of pedestrian motion from the initial moment of occurrence of the hazardous situation;

$\dot{x}_1, \dot{y}_1$ represent the projections of the velocity of the pedestrian's center of mass along the corresponding axes x and y during the period after the initial acceleration but before reaching a relatively constant motion speed. These parameters describe the intermediate phase of motion in which the pedestrian is still changing velocity before stabilization;

t_{p2} represents the time interval corresponding to motion at constant velocity;

$\varphi_{p1}, \varphi_{p2}$ represent the angular displacements during the first and the second time intervals t_{p1} and t_{p2};

$\ddot{\varphi}_{p1}$ represents the average angular acceleration of the pedestrian during the initial stage of motion;

$\dot{\varphi}_o$ represents the initial angular velocity of the pedestrian's center of mass at the moment the hazardous situation arises;

$\dot{\varphi}_2$ represents the steady state or transitional angular velocity at a later stage of motion.

This distance is determined under different motion conditions. Under real conditions the movement of the pedestrian may vary, as the pedestrian may accelerate, reduce the walking speed, or even stop before reaching the critical point. This creates a dynamic and difficult-to-predict traffic situation in which the driver is required to continuously reassess the risk of a potential collision.

The total distance $L(t)$ travelled by the vehicle from the moment the hazard is perceived until the vehicle reaches a complete stop is determined as follows:

$$L(t) = s_R + s_A + s_G + s_S \tag{8}$$

where

s_R is the distance travelled during driver reaction time t_1;

s_A is the distance travelled during the brake system activation time t_2;

s_G is the distance travelled during the time required for the braking force to increase from zero to its maximum value t_3;

s_S is the distance travelled during the time corresponding to full activation of the braking system t_4.

The distances in equation (8), taking into account the deceleration motion as well as the engine resistance forces and the rolling resistance forces of the wheels, are determined as follows:

$$\begin{aligned}
s_R &= \left(V_o.t_1 - \frac{1}{2}.a_r.t_1^2\right) && V_o \\
s_A &= \left(V_1.t_2 - \frac{1}{2}.a_r.t_2^2\right) && V_1 = V_o - a_r.t_1 \\
s_G &= \left(V_2.t_3 - \frac{1}{2}.a_r.t_3^2 - \frac{1}{6}.a_{max}.t_3^2\right) && V_2 = V_1 - a_r.t_2 \\
s_S &= \left(V_3.t_4 - \frac{1}{2}.(a_r + a_{max}).t_4^2\right) && V_3 = V_2 - a_r.t_3 - \frac{1}{2}.a_{max}.t_3 \\
&= \frac{V_3^2}{2.(a_r + a_{max})}
\end{aligned} \tag{9}$$

where

V_o is the initial velocity of the vehicle center of mass at the moment when the hazard is perceived;

t_1 is the driver reaction time;

t_2 is the brake system activation time;

t_3 is the time required for the braking force to increase to its maximum value;

 doi:10.20944/preprints202603.1262.v1

t_4 is the time corresponding to the full action of the braking system;

a_r is the deceleration caused by the engine resistance torque and the rolling resistance forces of the wheels;

a_{max} is the deceleration corresponding to the maximum braking force in the presence of an ABS system. The maximum braking deceleration can be estimated using the relationship $a_{max} = \mu g$, where μ is the coefficient of adhesion between the tire and the road surface. The friction coefficient is determined according to the Slip model [24, 25];

V_1 is the vehicle velocity at the end of the interval t_1;

V_2 is the vehicle velocity at the end of the interval t_2;

V_3 is the vehicle velocity at the end of the interval t_3.

The velocities V_1, V_2, and V_3 are determined sequentially from the kinematic relationships of motion with variable acceleration, taking into account the influence of resistance forces and the gradual increase of the braking force during each phase of the braking process [26].

For a given moment t_x, measured from the moment the hazard is perceived, the velocity $V(t_x)$ and the travelled distance $L(t_x)$ are determined depending on the phase of motion to which the moment belongs.

The total distance $L_1(t)$, travelled by the vehicle from the moment the hazardous situation arises for the driver until the vehicle reaches a complete stop is determined as

$$L_1(t) = s_x + s_R + s_A + s_G + s_S \tag{10}$$

where s_x, is an additional term representing the distance travelled during the time interval t_x before the hazard is perceived.

According to the analysis of equation (10) and the data obtained from judicial procedures, the following relationship is observed:

$$s_x > 0 \text{ or } s_x = 0 \tag{11}$$

It is evident that when the first inequality is satisfied, a delay in reaction occurs, which corresponds to the time t_x.

Particular interest for the analysis arises when the following condition is satisfied:

$$L_2(t) = s_A + s_G + s_S \tag{12}$$

From equation (12) it can be seen that the influence of the driver is practically absent, since vehicle control is assumed to be entirely performed by an automated system responsible for activating the braking and engine control actions.

Automated systems based on sensors and predictive algorithms are capable of identifying the hazard at an early stage, even before it is consciously perceived by the driver, and can initiate braking almost without delay. This means that under automated vehicle control the actually travelled distance does not include the additional distance covered during the human reaction time, a factor that often proves to be critical.

The improved dynamic model of vehicle motion (Figure 4) is formulated on the basis of six differential equations, three describing the linear displacement of the vehicle center of mass and three describing its angular rotations [27]. The analysis of the interaction between the vehicle and the pedestrian requires a systems engineering approach that integrates information related to driver behavior, vehicle motion dynamics, and environmental conditions [28,29].

doi:10.20944/preprints202603.1262.v1

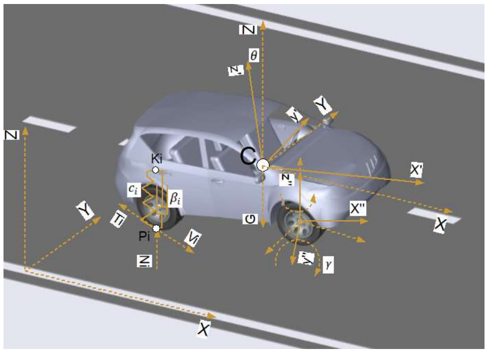

Figure 4. Dynamic vehicle model used for the simulation..

The generalized coordinates of the dynamic vehicle model are:

$x(t)$ is the position of the center of mass along the longitudinal axis of the fixed coordinate system;

$y(t)$ is the position of the center of mass along the lateral axis of the fixed coordinate system;

$z(t)$ is the position of the center of mass along the vertical axis of the fixed coordinate system;

$\varphi(t)$ is the rotation about the longitudinal axis;

$\theta(t)$ is the rotation about the lateral axis;

$\psi(t)$ is the rotation about the vertical axis.

Accordingly, the linear and angular velocities are obtained as $\dot{x}(t)$, $\dot{y}(t)$, $\dot{z}(t)$ representing the components of the linear velocity, and $\dot{\varphi}(t)$, $\dot{\theta}(t)$, $\dot{\psi}(t)$ representing the angular velocities.

The corresponding linear and angular accelerations are expressed as follows: $\ddot{x}(t)$, $\ddot{y}(t)$, $\ddot{z}(t)$ for the linear accelerations and $\ddot{\varphi}(t)$, $\ddot{\theta}(t)$, $\ddot{\psi}(t)$ for the angular accelerations.

Therefore, the gravitational force $\vec{G}$ acts along the Oz axis. The spatial arrangement of the car model is a rigid body supported by four elastic supports, which are marked by $K_i(i = 1 \div 4)$ (Figure 5).

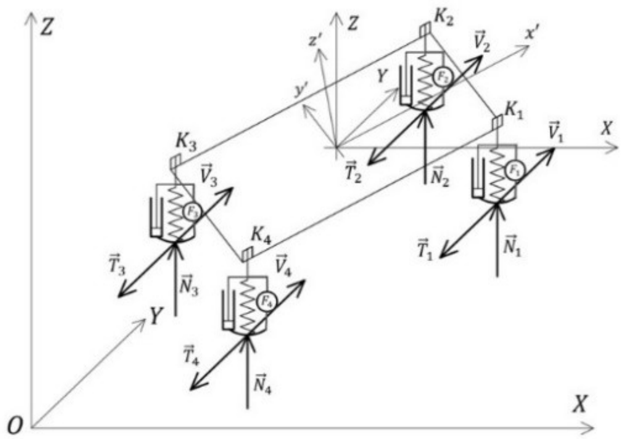

Figure 5. Model of forces acting on the vehicle during spatial motion considering tire and suspension elasticity.

$\vec{F}_i(i = 1 \div 4)$ is elastic force generated by the tire and suspension elasticity; $\vec{N}_i(i = 1 \div 4)$ is normal reaction at the tire–road contact point, corresponding to elastic force; $\vec{V}_i(i = 1 \div 4)$ is velocity of the contact point P_i in the road plane $0xy$; $\vec{T}_i(i = 1 \div 4)$ is friction force acting at the contact points that lies in the plane of the road $0xy$; $\vec{R}_i(i = 1 \div 4)$ is resistance force generated by the suspension damping elements; $c_i, \frac{N}{m}(i = 1 \div 4)$ suspension stiffness, taking into account both coefficient of elasticity of tires and suspension; $b_i, \frac{N \cdot s}{m}(i = 1 \div 4)$ coefficient of linear resistance.

 doi:10.20944/preprints202603.1262.v1

The vehicle motion based on the principles of kinetic energy and generalized forces is defined by six differential equations with six generalized coordinates. These equations are valid when the friction force follows Coulomb's law and wheel slip occurs without rolling.

The generalized forces and moments on the right-hand sides of the differential equations (13, 14) are determined by assuming that the absolute coordinate system has a vertical axis $0z$.

The differential equations governing the linear motion of the vehicle center of mass are formulated using three generalized coordinates defined in a selected Cartesian coordinate system.

$$[B_{ij}].\begin{bmatrix}\ddot{x}\\ \ddot{y}\\ \ddot{z}\end{bmatrix} = [F]$$

$$[F] = \begin{bmatrix}\sum_{i=1}^{4} F_{xi}\\ \sum_{i=1}^{4} F_{yi}\\ -G + \sum_{i=1}^{4} N_i - \sum_{i=1}^{4} R_i\end{bmatrix} \tag{13}$$

where $[B_{ij}]$ is the square matrix of the vehicle mass parameters of the vehicle, and $\begin{bmatrix}\ddot{x}\\ \ddot{y}\\ \ddot{z}\end{bmatrix}$ is the column vector of the projections of the accelerations of the vehicle center of mass. $[F]$ represents the column vector of the projections of the external forces.

The rotation of the vehicle is determined by the three Euler angles and the corresponding angular accelerations derived from them.

$$[A_{ij}].\begin{bmatrix}\ddot{\varphi}\\ \ddot{\psi}\\ \ddot{\theta}\end{bmatrix} = [M_{ij}]$$

$$[M_{ij}] = \begin{bmatrix}\sum_{i=1}^{4} M_{Ni} + \sum_{i=1}^{4} M_{Ri} + \sum_{i=1}^{4} M_{Fi} + \left(\sum -b_i \cdot \dot{q}_i^2\right) + \left(\sum -c_i \cdot \dot{q}_i \cdot \dot{q}_j\right)\\ \sum_{i=1}^{4} M_{Ni} + \sum_{i=1}^{4} M_{Ri} + \sum_{i=1}^{4} M_{Fi} + \left(\sum -b_j \cdot \dot{q}_j^2\right) + \left(\sum -c_j \cdot \dot{q}_j \cdot \dot{q}_k\right)\\ \sum_{i=1}^{4} M_{Ni} + \sum_{i=1}^{4} M_{Ri} + \sum_{i=1}^{4} M_{Fi} + \left(\sum -b_k \cdot \dot{q}_k^2\right) + \left(\sum -c_k \cdot \dot{q}_i \cdot \dot{q}_k\right)\end{bmatrix} \tag{14}$$

where $[A_{ij}]$ is a square matrix containing the coefficients associated with the angular accelerations expressed as functions of the inertia moments; $\begin{bmatrix}\ddot{\varphi}\\ \ddot{\psi}\\ \ddot{\theta}\end{bmatrix}$ is represents the column vector of angular accelerations corresponding to the selected generalized coordinates; $[M_{ij}]$ is the column vector representing the sum of moments of the normal reactions of the wheels, the moments of the damping forces, the moments of the friction forces, and the moments of the inertial forces; $\dot{q}$ represents the angular velocity corresponding to each generalized coordinate.

The system is solved in matrix form:

$$[Q] = [A]^{-1} \cdot [F] \tag{15}$$

where

doi:10.20944/preprints202603.1262.v1

$[Q]$ is the column vector of the unknown linear and angular accelerations of the vehicle center of mass;

$[A]^{-1}$ is the inverse of the coefficient matrix of the coefficients corresponding to the unknown variables;

$[F]$ is the column vector of generalized forces.

In addition to the differential equations describing the motion of the vehicle, the equations describing the motion of the wheels are also considered, which can be expressed as

$$[I_{\theta_i}].[\ddot{\theta}_i] = T_i.r_i + \{sign\,(\dot{\theta}_i).[M_{di} - f_i \cdot N_i - M_{si}]\}, \qquad i = 1 \div 4 \tag{16}$$

Figure 6 presents the dynamic model of the driving wheel, which can represent either two or four driven wheels.

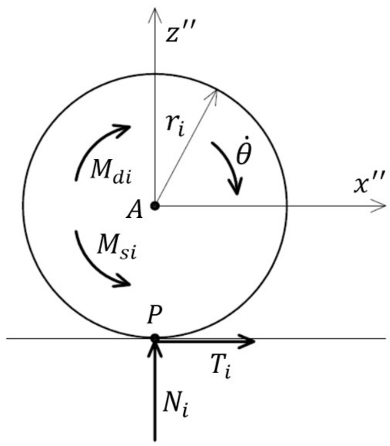

Figure 6. Dynamic model of the driven wheel.

The following notation is used: $\vec{r}_i$ is the radius of the wheel; f_i is the rolling resistance coefficient; $\vec{N}_i$ represents the normal reaction acting on the wheel; $[I_{\theta_i}]$ is the matrix of coefficients corresponding to the angular accelerations of the wheels; $[\ddot{\theta}_i]$ is the vector of angular velocities of the wheels.

In the context of risk assessment in road traffic accidents, it is important to realistically model the variation in pedestrian velocity. In such cases time dependent accelerations are considered, where $a(t)$ can be described using a function that may be linear, exponential, or based on empirical data.

3. Numerical Investigation

A numerical experiment was conducted using a dynamic model of a passenger car based on known technical characteristics, including inertial parameters, vehicle mass, elastic and damping properties of the suspension, as well as the geometric dimensions of the vehicle. The initial conditions of the differential equations describing wheel motion were also incorporated into the differential equations of vehicle motion. The analysis was performed for an initial velocity of the vehicle center of mass of 70 km/h.

A transverse pedestrian crossing scenario was examined, in which the pedestrian enters the roadway from the right side relative to the direction of vehicle motion and moves with an approximately constant speed of 7.2 km/h. The trajectory corresponds to a typical transverse crossing scenario, with the initial appearance of the pedestrian detected within the right peripheral vision zone of the driver, an area generally associated with minimal delay in the perception of an emerging hazard.

The main focus of this numerical experiment is the assessment of risk and the influence of the human factor on the interpretation of the linguistic variables characterizing the road environment and the vehicle, as well as on the actions taken by the driver in response to pedestrian behavior.

 doi:10.20944/preprints202603.1262.v1

The analysis of the examined cases from judicial practice shows that the drivers involved in road traffic incidents are predominantly male. For this reason, a targeted study of the reaction time of male drivers from different age groups was conducted using a driving simulator, presented in Figure 7. This approach provides the possibility to evaluate the real responses of this group of drivers and to compare them with the data derived from court cases, thereby achieving greater consistency between the empirical results and the dynamic modeling.

Figure 7. Driving simulator used to measure driver reaction time.

The results of the reaction time study are presented in Table 1, where the ranges corresponding to each age group are shown. Reaction time was recorded using the capabilities of the simulator through three consecutive trials for each participant. The measured intervals correspond to the time between the appearance of a pedestrian hazard and the driver's response action, namely pressing the brake pedal. The experiment was conducted under three different experimental conditions corresponding to the categories expected hazard, unexpected hazard, and surprise.

Participants were presented with scenarios in which a pedestrian suddenly entered the roadway under different conditions of visibility, vehicle speed, and road surface adhesion. In this way responses were elicited under conditions that closely resemble real traffic situations, which made it possible to evaluate the influence of age and expectancy on driver reaction time. The obtained data complement the information derived from judicial practice with controlled experimental observations and provide quantitative parameters for the dynamic model necessary for a more accurate assessment of accident risk.

The objective of the experimental study is not to establish universal reaction time values but to provide empirical parameters comparable to the analyzed judicial cases. In this way a better correspondence is achieved between real scenarios derived from judicial practice and the input parameters of the dynamic model.

Table 1. Driver reaction time intervals for different age groups.

№	Age group (years)	Driver reaction time intervals [s]		
		Reaction time interval in surprise conditions [s]	Reaction time interval in unexpected hazard conditions [s]	Reaction time interval in expected hazard conditions [s]
1	up to 30	0.93–1.20	1.01–1.08	0.76–0.87
2	30–40	1.11–1.38	1.02–1.20	0.96–1.02
3	40–50	1.40–1.85	1.05–1.25	1.02–1.20
4	50–60	2.23–2.25	1.44–1.48	1.15–1.21
5	over 60	2.32–2.36	1.60–1.72	1.23–1.35

 doi:10.20944/preprints202603.1262.v1

Within the framework of this scenario, the main components of the reaction process were considered, including a driver reaction time of 1 s, a brake system activation time of 0.2 s, and a time of 0.4 s required to reach the maximum braking deceleration. This indicates that the driver was particularly attentive or that the hazard was perceived in a timely manner, allowing the driver to react at the moment the pedestrian began to enter the roadway (Figs. 8–10).

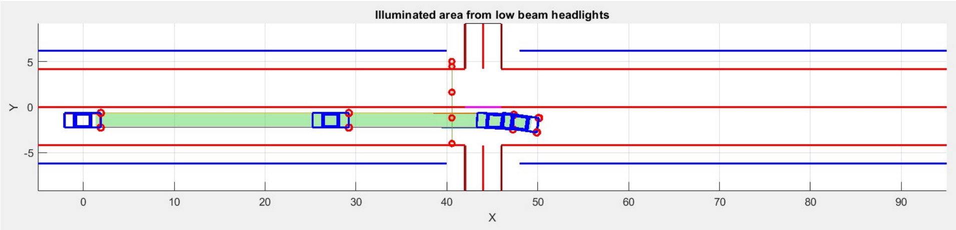

Figure 8. Discrete positions of the vehicle and the pedestrian during motion under timely hazard perception conditions.

The obtained risk assessment is used as an input parameter for the simulation model, where it serves as a logical criterion for activating different operating modes, including the formation of the hazardous stopping zone, the selection of a specific scenario, and the activation of emergency braking when a defined threshold is reached. The data obtained from the driving simulator determine the parameter reaction time, which participates in the calculation of the hazardous stopping zone and in defining the moment at which the model switches from motion to braking. In this way the risk assessment determines the moment of activation of the simulation mechanisms, while the measured reaction times influence the calculated stopping distances and the preventability of the accident.

The analysis was carried out through the numerical solution of the differential equations of motion, taking into account the influence of the human factor on the braking process. Figure 8 presents the discrete relative positions of the vehicle and the pedestrian during their motion. The vehicle and the pedestrian are visualized at several different moments of their interaction. The action on the brake pedal and the achievement of maximum braking efficiency following timely hazard perception determine the driver's ability to avoid the collision.

Figure 9 presents the time variation of the engine torque and the braking torque $M_{s\,max}$, It can be observed that up to $t = 1.2\ s$ the braking torque remains zero. After this moment a rapid increase occurs, reaching the maximum braking force within approximately 0.4 s. This behavior indicates activation of the braking system with full efficiency, which leads to intensive braking until the vehicle reaches a complete stop.

The obtained dynamics are indicative of an emergency braking scenario in which the system responds in a timely manner depending on the hazard perception time and the driver reaction time. The projections of the velocity of the pedestrian and the vehicle center of mass as functions of time are also presented.

Preprints.org (www.preprints.org) | NOT PEER-REVIEWED | Posted: 17 March 2026 doi:10.20944/preprints202603.1262.v1

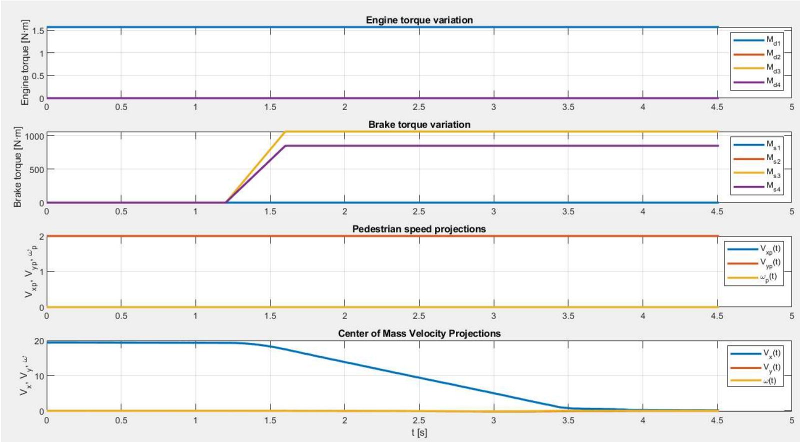

Figure 9. Time variation of engine torque, braking torque, and velocity projections of the pedestrian and the vehicle center of mass.

Figure 10 presents the trajectories of the vehicle and the pedestrian. From the first graph it can be seen that the projection of the pedestrian center-of-mass velocity along the Y-axis remains constant. The projection of the vehicle center-of-mass velocity along the X-axis up to $t = 1.2\ s$ decreases only slightly. Within this time interval the driver perceives the hazard and initiates braking. Until the moment when the deceleration begins to increase, the vehicle operates in the engine forced-idle regime.

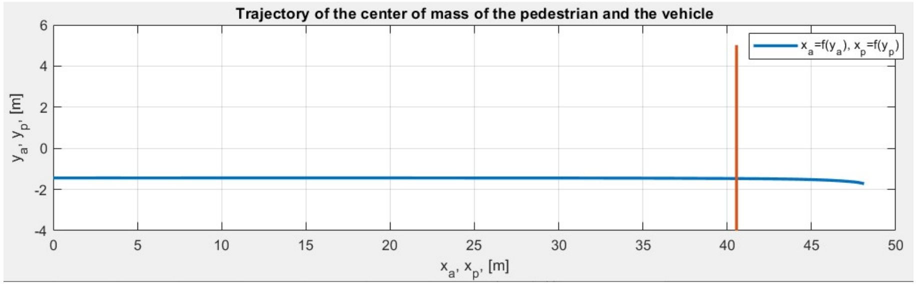

Figure 10. Trajectories of the vehicle and the pedestrian.

The results of the first numerical simulation show that when the moment of hazard occurrence and the moment of hazard perception coincide with the moment the pedestrian enters the roadway, the driver has a real opportunity to prevent a road traffic accident. The analysis confirms that when the reaction begins at the initial critical moment, the available distance and time window are sufficient for effective activation of the braking system, which allows safe avoidance of a collision between the vehicle and the pedestrian.

The level of risk is particularly high in situations involving approach to an intersection when a pedestrian enters the traffic area from the continuation of the sidewalk. Under such conditions even minimal delay in perception due to visual distraction, cognitive workload, or inattention may lead to an accident. Despite optimal technical characteristics of the vehicle, human perception remains a critical factor in collision avoidance.

Therefore, timely detection of a pedestrian within the critical zone and immediate initiation of braking actions are essential. This emphasizes the need for the implementation of perception assistance systems and automated response mechanisms that can compensate for risks arising from the human factor in environments with a high concentration of vulnerable road users.

The second model examines the analysis of the vehicle motion with a reaction delay time of 1 s (Figures 11 and 12). Similarly, a driver reaction time of 1.0 s is assumed, a braking system activation time of 0.2 s, and a braking force build-up time of 0.4 s.

 doi:10.20944/preprints202603.1262.v1

Figure 11 presents discrete positions of the vehicle and the pedestrian relative to the initial moment of hazard occurrence and perception. The movement corridor zone, shown in green, indicates the time delay in hazard perception, while the delayed motion regime demonstrates that the vehicle and the pedestrian cannot avoid a collision.

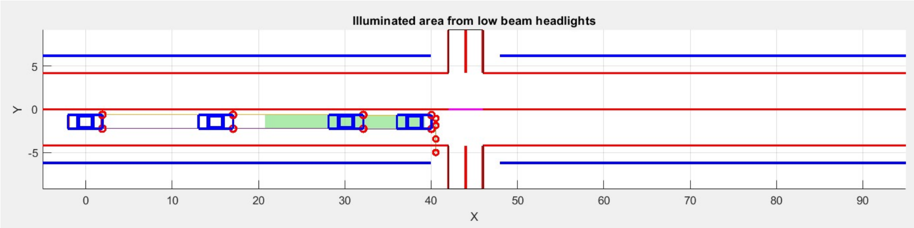

Figure 11. Discrete positions of the vehicle and the pedestrian at the moment of hazard perception.

Figure 12 presents the time variation of the braking torque M_{smax}. It can be observed that the braking torque remains zero up to $t = 2.2\ s$ the braking torque remains zero. After this moment, a rapid increase occurs, reaching the maximum braking torque within approximately 0.4 s.

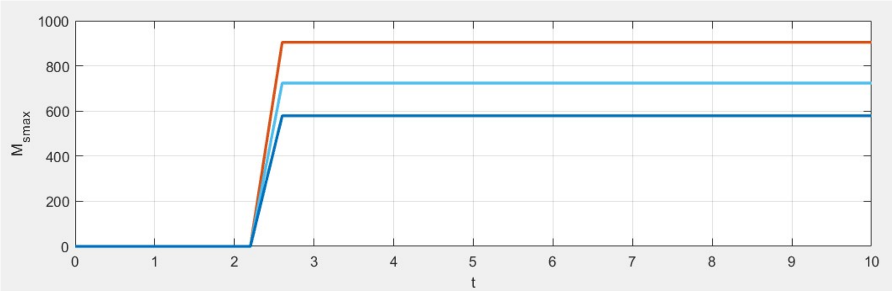

Figure 12. Time variation of the braking torque.

Figures 13 and 14 present the time variation of the velocity projections of the center of mass of the pedestrian and the vehicle. For the pedestrian, a relatively constant velocity component is observed along the Y-axis.

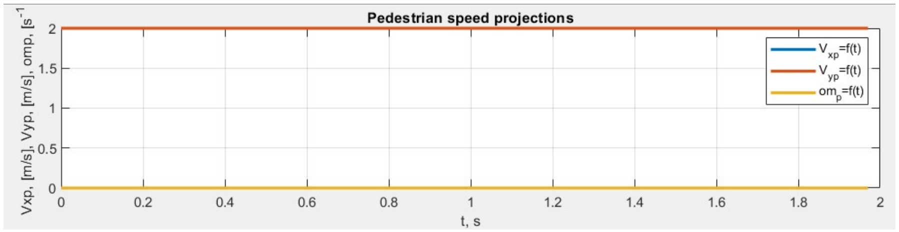

Figure 13. Time variation of the velocity projections of the pedestrian center of mass.

Preprints.org (www.preprints.org) | NOT PEER-REVIEWED | Posted: 17 March 2026 doi:10.20944/preprints202603.1262.v1

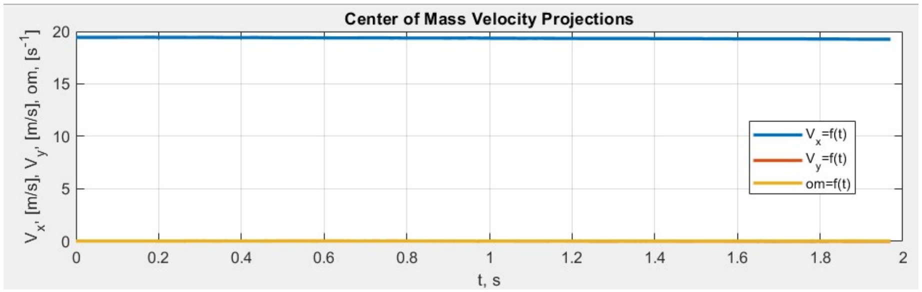

Figure 14. Time variation of the velocity projections of the vehicle center of mass.

The projection of the vehicle velocity along the X-axis remains constant, which indicates that the braking system is not activated. The collision occurs while the vehicle center-of-mass velocity remains unchanged until the moment of impact.

Figure 15 presents the trajectories of the center of mass of the vehicle and the pedestrian. A key aspect of the analysis is the driver reaction delay of 1 s, which, considering the vehicle dimensions, determines the impossibility of preventing the collision.

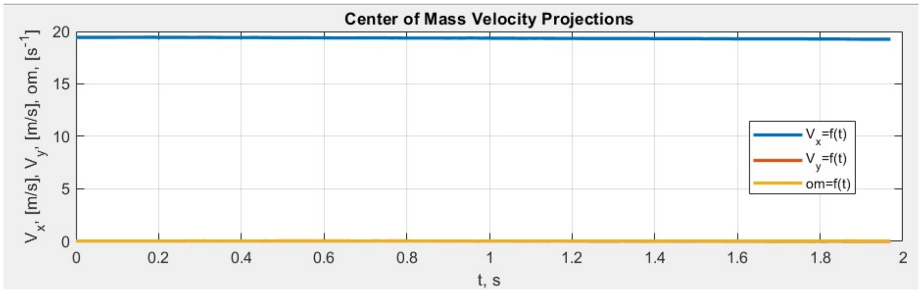

Figure 15. Trajectories of the centers of mass of the vehicle and the pedestrian.

The conclusions from the second numerical model, in which the driver reacts with a delay of approximately 1.0 s after the hazard occurs, clearly show that even a minimal distraction of attention and a slight delay in reaction may lead to a collision between the vehicle and the pedestrian.

The obtained results demonstrate that even a delay in hazard perception of approximately 1 s may result in the loss of the technical capability to prevent the collision. This effect is caused by the additional distance travelled at an approximately constant speed before the braking process begins. As a consequence, the vehicle covers an additional distance prior to braking, which significantly reduces the probability of stopping before the vehicle enters the pedestrian crossing corridor.

This scenario clearly illustrates the inherent vulnerability of the driver–vehicle system in situations involving momentary distraction, fatigue, or reduced concentration. A similarly elevated level of risk may arise under conditions of limited visibility, when approaching pedestrian crossings, or in the presence of distracting lateral visual stimuli. Under such circumstances, even a brief loss of attention lasting only fractions of a second may lead to severe consequences.

The analysis therefore confirms that the human factor plays a dominant role in accident risk formation, regardless of the technical characteristics of the vehicle. Effective accident prevention in such situations requires either the elimination of driver reaction delay or its compensation through automated early warning and emergency braking systems capable of operating within millisecond response times.

The third scenario analyzes hazard management in the event of a potential collision through an automated system for controlling the braking and engine torque. The numerical experiment is performed at a vehicle speed of 70 km/h and without the influence of the human factor (Figures 16–

 doi:10.20944/preprints202603.1262.v1

17). The simulation is carried out under conditions of increased risk of collision with a pedestrian in order to analyze the effectiveness of the automated system.

Figure 16 presents discrete positions of the relative motion between the vehicle and the pedestrian. It can be observed that they pass without collision, while the hazard assessment is fully automated and does not depend on the human factor.

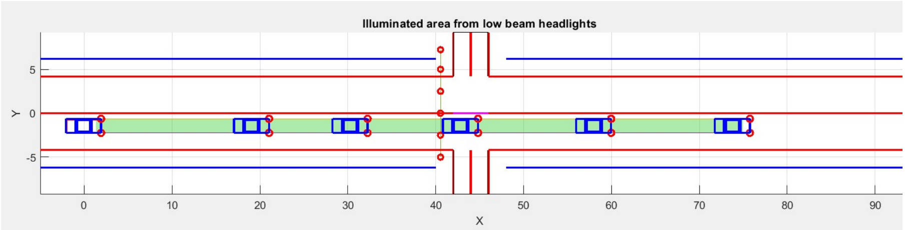

Figure 16. Discrete positions of the vehicle and the pedestrian at the moment of hazard perception.

Figure 17 shows the time variation of engine torque and braking torque under automated hazard evaluation. The activation of the braking torque in the presented model is based on a predictive assessment of the risk of collision with a pedestrian obtained through simulation of the future trajectories of the traffic participants. Braking intervention is activated when the predicted position of the pedestrian enters the hazardous zone in front of the vehicle in front of the vehicle and the and the estimated time to collision indicates a critical situation.

Depending on the remaining time before the potential incident, a proportional coefficient governing the increase of braking torque is determined, which ensures adaptive and progressive activation of the braking process. The model also incorporates ABS control logic which, through slip filtering, ensures vehicle stability and optimal distribution of braking force between the wheels.

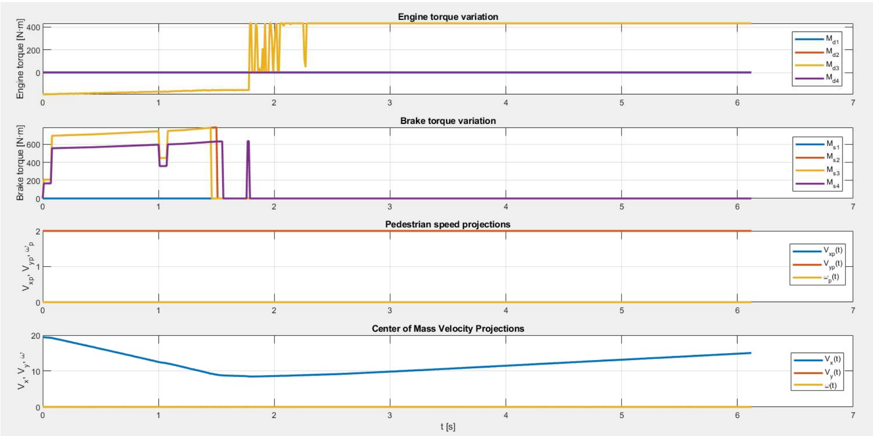

Figure 17. Time variation of engine torque, braking torque, and velocity projections of the centers of mass of the pedestrian and the vehicle.

Additional velocity projections of the center of mass of the vehicle and the pedestrian are also presented. According to the graph, when a hazard is detected the projection of the velocity of the vehicle center of mass along the X axis decreases with variable deceleration as a result of the applied braking torque. After the hazard has passed at $t = 1.8\ s$, the velocity of the center of mass begins to increase again, indicating that the risk has been eliminated.

Figure 18 presents the trajectories of the vehicle and pedestrian centers of mass. A key aspect of the analysis is the driver reaction delay of 1 s, which, considering the vehicle dimensions, determines the impossibility of preventing the collision.

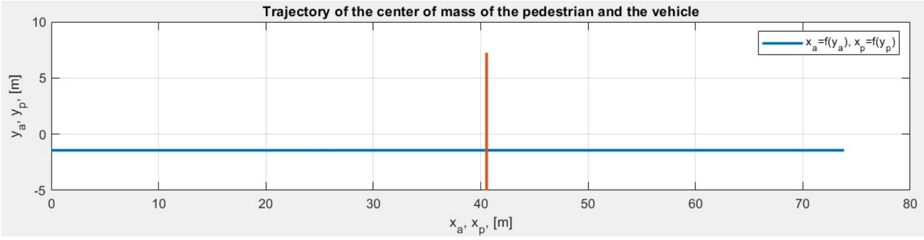

Figure 18. Trajectories of the vehicle and pedestrian centers of mass.

In the developed model, the engine torque control mode is activated when safe conditions for acceleration occur, taking into account the current motion and position of the vehicle relative to the pedestrian. Engine torque is applied when the emergency braking mode is inactive and the collision risk has been eliminated. When these conditions are satisfied simultaneously, the model activates the acceleration command by supplying engine torque. This ensures a smooth transition from braking to driving while maintaining traffic safety.

The analysis of the third numerical simulation, in which the vehicle moves with an initial speed of 70 km/h and the response is fully controlled by an automated system, clearly demonstrates that even under adverse conditions characterized by higher kinetic energy and a shortened reaction time interval the collision can be successfully prevented. The immediate intervention of the braking system, activated without delay, together with its ability to adapt the braking force in real time, is crucial for avoiding the incident.

This result highlights the significant advantage of intelligent automated emergency braking systems which, through continuous processing of sensor information and algorithmic risk assessment, can initiate corrective actions on a millisecond time scale. Such responsiveness is practically unattainable for human perception and motor response, particularly in situations involving visual or cognitive limitations.

Despite the high level of risk caused by vehicle speed and the immediate hazard, the effectiveness of the automated system remains high due to the elimination of delays inherent to the human factor. The obtained results clearly confirm that the implementation of such technologies significantly increases the probability of successfully avoiding a collision even in critical situations where human intervention would be inadequate or delayed.

Considering these circumstances, the need for the widespread implementation of automated systems for controlled risk management becomes not only a technological priority but also a strategic measure for improving road safety, particularly in urban environments with intensive pedestrian presence.

It should be noted that the developed model is based on the analysis of court cases and experimental data related to driver reaction time, which implies certain limitations. Some parameters have been determined through expert interpretation of judicial practice and may vary depending on the specific conditions of the road environment and the behavior of traffic participants. Nevertheless, the proposed methodology enables systematic identification of the key factors influencing the risk of pedestrian related road traffic accidents and provides a basis for further development of dynamic models for risk assessment and risk management.

4. Results and Discussion

As a result of the numerical investigations, a multifactor assessment of the factors influencing the occurrence of pedestrian-involved road traffic accidents was performed. Real cases occurring under different meteorological conditions were analyzed, characteristics of the road infrastructure, and technical conditions of the vehicles were analyzed, as well as different behavioral responses of both the driver and the pedestrian.

The analysis considered key dynamic parameters such as vehicle speed, the moment of hazard occurrence, and the driver's perception time of the pedestrian. These parameters allow a more accurate assessment of the conditions under which the risk of a road traffic accident is formed.

The main objective of this study is to determine risk levels through the application of an integrated multifactor approach. A methodology for the identification, classification, and quantitative evaluation of the main risk factors has been developed. In this context, a system of linguistic variables describing critical characteristics of the transport system and the behavior of road users is proposed.

The methodology is based on data extracted from court decisions related to specific road traffic accidents, on the basis of which the values of the linguistic variables were determined. These variables are structured into three main groups.

The first group includes 11 variables describing road infrastructure and meteorological conditions. The second group contains 5 variables describing the technical characteristics of the vehicle. The third group includes 15 variables related to the behavior and condition of the driver.

This structure enables the evaluation of the individual contribution of each variable and their combined influence on the risk of road traffic accidents.

For the purposes of the quantitative analysis, each considered case is represented by a vector of linguistic variable values in the following form:

$$\begin{gathered}\Omega_1 = [10,20,60,10,30,10,10,10,60,40,10,75,60,40,90,\\ 10,40,10,20,30,70,50,60,50,20,10,30,60,60,60,60]\end{gathered} \tag{17}$$

The vector of the maximum values of the linguistic variables, arranged according to the same groups, is given as follows:

$$\begin{gathered}\Omega_{max} = [90,60,70,90,90,50,70,80,80,80,90,90,80,80,70,\\ 90,90,90,90,90,80,90,90,90,90,90,90,90,90,90,90]\end{gathered} \tag{18}$$

Based on the ratio between the actual and maximum values of the linguistic variables, the weighted risk values of the corresponding terms are calculated.

For the first group, the following expression is obtained:

$$S_{1,1} = \frac{\omega_1}{\sum_{i=1}^{11}\omega_{max,1}}.T_1.100 = \frac{\omega_1}{\sum_{i=1}^{11}\omega_{max,1}}.\frac{\sum_{i=1}^{11}\omega_{i,1}}{\sum_{i=1}^{31}\omega_i}.100 = \frac{10}{870}.\frac{270}{1175}.100 = 0.264\% \tag{19}$$

Similarly, for the terms of the second and third groups, the following expressions are obtained:

$$\begin{gathered}S_{12,2} = \frac{\omega_{12}}{\sum_{i=12}^{16}\omega_{max,2}}.T_2.100 = \frac{\omega_{12}}{\sum_{i=12}^{16}\omega_{max,2}}.\frac{\sum_{i=12}^{16}\omega_{i,2}}{\sum_{i=1}^{31}\omega_i}.100 = \frac{75}{440}.\frac{275}{1175}.100 = 3.989\%\\ S_{17,3} = \frac{\omega_{17}}{\sum_{i=17}^{31}\omega_{max,3}}.T_3.100 = \frac{\omega_{17}}{\sum_{i=17}^{31}\omega_{max,3}}.\frac{\sum_{i=17}^{31}\omega_{i,3}}{\sum_{i=1}^{31}\omega_i}.100 = \frac{40}{1340}.\frac{630}{1175}.100 = 1.601\%\end{gathered} \tag{20}$$

After calculating the weighted values of all terms, the results are aggregated by groups, allowing the determination of the partial risk for each group of factors.

For the first analyzed case, the following values are obtained:

$$\begin{gathered}S_1 = \sum_{i=1}^{11} S_{1,i} = 7.131\%, \qquad S_2 = \sum_{i=12}^{16} S_{2,i} = 14.628\%,\\ S_3 = \sum_{i=17}^{31} S_{3,i} = 25.208\%\end{gathered} \tag{21}$$

The overall risk assessment for the first analyzed case is determined as the sum of the partial risks of the three groups of factors:

$$T_1 = S_1 + S_2 + S_3 \tag{22}$$

$$T_1 = 7.131 + 14.628 + 25.208 = 46.97\%$$

The obtained value characterizes the integrated level of risk in the considered case, taking into account the combined influence of the factors from the three main groups. The analysis of the partial risks indicates that the largest contribution to the formation of the overall risk comes from the third group of factors related to driver behavior and condition, whose relative share reaches 25.208%.

A significant contribution is also observed for the second group of factors describing the technical parameters of the vehicle, where the partial risk value is 14.628%. A relatively smaller contribution is associated with the first group of factors related to road infrastructure and meteorological conditions, where the partial risk amounts to 7.131%.

The obtained distribution of risk confirms the dominant role of the human factor in the occurrence of pedestrian-involved road traffic accidents. Nevertheless, the influence of vehicle technical characteristics and road environmental conditions also plays a significant role on the overall level of risk and should be considered within the framework of an integrated multifactor analysis.

The first pie chart in Figure 19a shows the distribution of risk levels for the elements “road”, “meteorological conditions”, and “vehicle”. The analysis shows that the share of cases with a the share of cases with a risk level up to 40 units is 68.6%, while the share within the interval of 41 to 70 units is 18.8%, and values above 71 units account for 12.5%.

The second pie chart in Figure 19b illustrates the risk levels associated with driver behavior. It can be observed that in 46.7% of the cases the risk level is up to 40 units, in 53.3% the risk falls within the interval of 41 to 70 units, while values above 71 units are not observed.

The relative distribution of the factors indicates that the share of the elements “road” and “meteorological conditions” is 23.0%, the share of the element “vehicle” is 23.4%, and the share of the element “driver” is 53.6%, with the total equal to 100%.

The overall integrated risk assessment for the considered case is 46.97%.

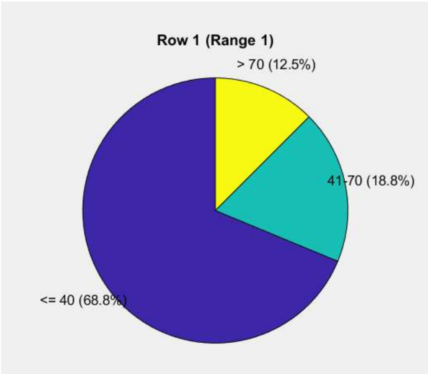

(**a**)

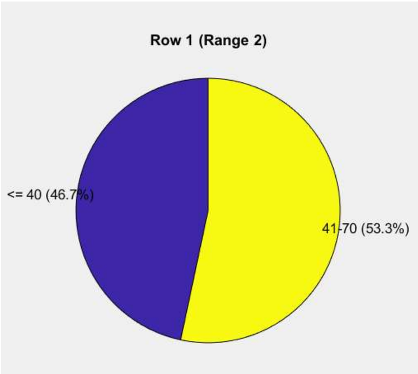

(**b**)

Figure 19. Distribution of weighted risk levels corresponding to the integrated risk value of 46.97%. (a) weight levels for the elements road and vehicle; (b) driver behavior.

Similarly to the presented analysis, two additional cases from the examined set of more than 100 road traffic accidents were considered.

The vector of linguistic variables corresponding to the minimum risk assessment relative to the first case has the following form:

$$\Omega_{min} = [10,20,60,10,30,10,10,10,60,40,10,75,60,40,\\ 90,10,40,10,20,30,10,50,30,50,20,10,30,60,60,60,60] \quad (23)$$

The relative distribution of the factors indicates that the share of the elements “road” and “meteorological conditions” is 24.9%, the share of the element “vehicle” is 25.4%, and the share of the element “driver” is 49.8%, with the total equal to 100%. The overall integrated risk assessment for the considered case is 43.62%. The difference of approximately three percentage points compared to the

Preprints.org (www.preprints.org) | NOT PEER-REVIEWED | Posted: 17 March 2026 doi:10.20944/preprints202603.1262.v1

first case is mainly attributed to the influence of the moment of hazard occurrence and the driver's reaction time, which significantly affects the possibility of preventing the road traffic incident.

The vector of linguistic variables for the second case has the following form:

$$\Omega_2 = [20,20,80,10,60,20,10,10,60,70,10,60,40,40,\\ 90,10,40,10,20,30,80,90,90,70,60,50,30,80,70,80,70] \quad (24)$$

The weighted risk values for each term within the groups are determined according to the following relationship:

$$S_{1,1} = \frac{\omega_1}{\sum_{i=1}^{11} \omega_{max,1}}.T_1.100 = \frac{\omega_1}{\sum_{i=1}^{11} \omega_{max,1}}.\frac{\sum_{i=1}^{11} \omega_{i,1}}{\sum_{i=1}^{31} \omega_i}.100 = \frac{20}{870}.\frac{370}{1480}.100 = 0.575\% \quad (25)$$

Similarly, for the terms of the second and third groups, the following expressions are obtained:

$$S_{12,2} = \frac{\omega_{12}}{\sum_{i=12}^{16} \omega_{max,2}}.T_2.100 = \frac{\omega_{12}}{\sum_{i=12}^{16} \omega_{max,2}}.\frac{\sum_{i=12}^{16} \omega_{i,2}}{\sum_{i=1}^{31} \omega_i}.100 = \frac{60}{410}.\frac{240}{1480}.100 = 2.211\%$$

$$S_{17,3} = \frac{\omega_{17}}{\sum_{i=17}^{31} \omega_{max,3}}.T_3.100 = \frac{\omega_{17}}{\sum_{i=17}^{31} \omega_{max,3}}.\frac{\sum_{i=17}^{31} \omega_{i,3}}{\sum_{i=1}^{31} \omega_i}.100 = \frac{40}{1340}.\frac{870}{1480}.100 = 1.755\% \quad (26)$$

After calculating the weighted values of all terms, the results are summed within each group, which allows the determination of the partial risk associated with the corresponding group of factors. For the considered case, the group sums are as follows:

$$S_1 = \sum_{i=1}^{11} S_{1,i} = 10.632\%, \qquad S_2 = \sum_{i=12}^{16} S_{2,i} = 8.845\%,$$

$$S_3 = \sum_{i=17}^{31} S_{3,i} = 38.166\% \quad (27)$$

The overall risk value for the considered case is calculated as the sum of the partial risks of the three groups of factors:

$$T_1 = S_1 + S_2 + S_3$$
$$T_1 = 10.632 + 8.845 + 38.166 = 57.64\% \quad (28)$$

The first pie chart in Figure 20a shows the distribution of risk levels for the elements "road", "meteorological conditions", and "vehicle". The analysis shows that the share of cases with a risk level up to 40 units is 62.5%, while the share within the range of 41 to 70 units is 25.0%, and values above 70 units account for 12.5%.

Figure 20b illustrates the risk levels associated with driver behavior. It is observed that in 33.3% of the cases the risk level is up to 40 units, in 33.3% it falls within the interval of 41 to 70 units, and in 33.4% the values exceed 71 units.

The relative distribution of the factors indicates that the share of the elements "road" and "meteorological conditions" is 25.0%, the share of the element "vehicle" is 16.2%, and the share of the element "driver" is 58.8%, with the total equal to 100%. The overall integrated risk assessment for the considered case is 57.64%.

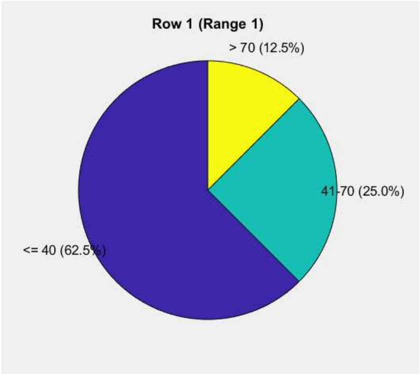

(a)

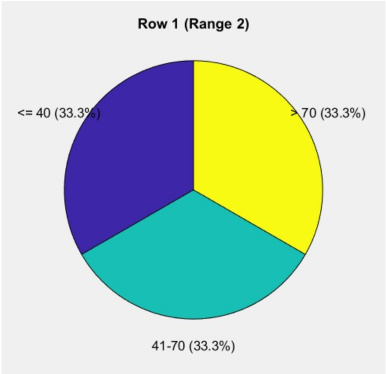

(b)

Figure 20. Distribution of weighted risk levels corresponding to the integrated risk value of 57.64%. (a) weight levels for the elements road and vehicle; (b) driver behavior.

A third analyzed case is also presented, in which the vector of linguistic variables has the following form:

$$\Omega_3 = [70,20,60,25,30,20,70,80,80,70,75,60,40,40,\\ 90,10,60,10,20,30,70,70,90,70,20,80,90,60,60,80,70] \quad (29)$$

The weighted risk values for each term within the groups are calculated according to the following relationship:

$$S_{1,1} = \frac{\omega_1}{\sum_{i=1}^{11} \omega_{max,1}}.T_1.100 = \frac{\omega_1}{\sum_{i=1}^{11} \omega_{max,1}}.\frac{\sum_{i=1}^{11} \omega_{i,1}}{\sum_{i=1}^{31} \omega_i}.100 = \frac{70}{870}.\frac{600}{1720}.100 = 2.807\% \quad (30)$$

Similarly, the following values are obtained for the terms of the second and third groups:

$$S_{12,2} = \frac{\omega_{12}}{\sum_{i=12}^{16} \omega_{max,2}}.T_2.100 = \frac{\omega_{12}}{\sum_{i=12}^{16} \omega_{max,2}}.\frac{\sum_{i=12}^{16} \omega_{i,2}}{\sum_{i=1}^{31} \omega_i}.100 = \frac{60}{440}.\frac{240}{1720}.100 = 1.903\%$$

$$S_{17,3} = \frac{\omega_{17}}{\sum_{i=17}^{31} \omega_{max,3}}.T_3.100 = \frac{\omega_{17}}{\sum_{i=17}^{31} \omega_{max,3}}.\frac{\sum_{i=17}^{31} \omega_{i,3}}{\sum_{i=1}^{31} \omega_i}.100 = \frac{60}{1340}.\frac{880}{1720}.100 = 2.291\% \quad (31)$$

After calculating the weighted values of all terms, the results are summed within each group, allowing the determination of the partial risk for each group of factors. The obtained group sums are as follows:

$$S_1 = \sum_{i=1}^{11} S_{1,i} = 24.058\%, \qquad S_2 = \sum_{i=12}^{16} S_{2,i} = 7.611\%,$$
$$S_3 = \sum_{i=17}^{31} S_{3,i} = 33.599\% \quad (32)$$

The overall risk assessment for the considered case is determined as the sum of the partial risks of the three factor groups:

$$T_1 = S_1 + S_2 + S_3$$
$$T_1 = 24.058 + 7.611 + 33.599 = 65.27\% \quad (33)$$

The first pie chart in Figure 21a shows the distribution of risk levels for the elements “road”, “meteorological conditions”, and “vehicle”. The analysis shows that the share of cases with a risk level up to 40 units is 43.8%, while the share within the range of 41 to 70 units is 31.3%, and values above 70 units account for 25.0%.

The second pie chart in Figure 21b illustrates the risk levels associated with driver behavior. It can be observed that in 26.7% of the cases the risk level is up to 40 units, in 46.7% it falls within the range of 41 to 70 units, and in 28.7% the values exceed 71 units.

The relative distribution of the factors indicates that the share of the elements "road" and "meteorological conditions" is 34.9%, the share of the element "vehicle" is 14.0%, and the share of the element "driver" is 51.1%, with the total equal to 100%. The overall integrated risk assessment for the considered case is 65.27%.

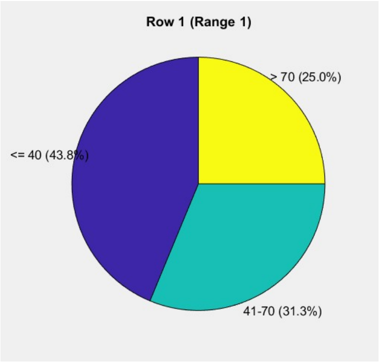

(**a**)

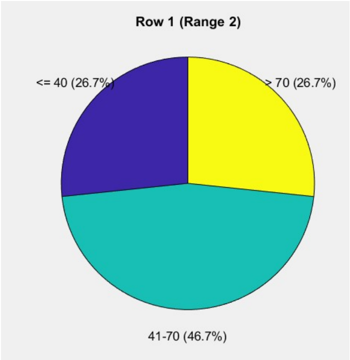

(**b**)

Figure 21. Distribution of weighted risk levels corresponding to the integrated risk value of 65.27%. (a) weight levels for the elements road and vehicle; (b) driver behavior.

Based on the expert structuring of the analyzed cases and the application of the proposed risk assessment methodology, eleven consecutive risk levels were identified. These levels are defined through an integrated quantitative evaluation of linguistic variables of the linguistic variables related to the road environment, the technical characteristics of the vehicle, and driver behavior. Such stratification allows the systematization of the observed cases and allows a more detailed analysis of the factors contributing to the occurrence of pedestrian-involved road traffic accidents.

The analysis of the obtained results reveals a clear relationship between the increase in integrated risk and the growing contribution of the human factor. At lower risk levels, factors related to the road environment and the technical characteristics of the vehicle tend to dominate. As the integrated risk values increase, particularly in the range above 50%, driver behavior emerges as the primary determining element in the formation of the overall risk assessment.

The first risk level includes values up to 39.99% and is characterized by a predominance of low-risk linguistic variables. Within this range, driver behavior remains stable, while the observed deviations are isolated and do not significantly affect the overall safety assessment.

The second and third risk levels, corresponding to the ranges of 40.00–42.99% and 43.00–45.99%, are characterized by a gradual increase in the proportion of variables associated with a moderate level of risk. However, values corresponding to the high-risk category remain limited, indicating that driver behavior still remains under relatively stable control.

The fourth and fifth risk levels, corresponding to the ranges of 46.00–48.99% and 49.00–51.99%, show a progressive increase in risk values, particularly in the variables associated with driver behavior. At these levels, a higher proportion of terms belonging to the moderate risk range is observed, which leads to an increase in the overall integrated risk value.

The sixth and seventh risk levels, covering the ranges of 52.00–54.99% and 55.00–57.99%, are characterized by a noticeable increase in risk values both in driver behavior and in some factors related to the road environment. Within this range, the share of variables belonging to the high-risk class increases, indicating a strengthening of the critical factors contributing to risk formation.

The eighth and ninth risk levels, corresponding to the ranges of 58.00–60.99% and 61.00–63.99%, demonstrate a clear shift of risk values toward the moderate and high-risk categories. At these levels,

Preprints.org (www.preprints.org) | NOT PEER-REVIEWED | Posted: 17 March 2026 doi:10.20944/preprints202603.1262.v1

driver behavior becomes the dominant factor contributing to the increase in integrated risk, while the influence of the road environment and vehicle technical characteristics remains relatively limited.

The tenth risk level covers the range of 64.00–66.99% and is characterized by the predominance of values within the high-risk category, particularly for linguistic variables associated with driver behavior. In these cases, significant deviations in driver reactions and actions are observed when hazardous situations arise.

The eleventh risk level includes values above 70.00% and represents the highest risk category. At this level, a clear dominance of behavioral factors and a significant proportion of variables belonging to the high-risk category are observed. This level is characterized by critical manifestations in driver behavior and a substantially increased probability of road traffic accidents.

The eleven risk levels were established based on the analysis of 105 real court cases, in which recurring combinations of factors related to driver behavior, road environment characteristics, and accident dynamics were identified. These levels reflect empirically observed patterns of criticality in judicial practice and provide a structured framework for the systematic risk assessment of pedestrian-involved road traffic accidents.

The obtained results, combined with the analysis of more than 100 court decisions, indicate that driver behavior remains the dominant factor in the formation of risk in pedestrian-involved road traffic accidents. At the same time, the influence of the road environment and the technical characteristics of the vehicle appears to be significantly more limited.

The results of the dynamic simulations were analyzed using the proposed risk assessment methodology based on linguistic variables and Kernel Density Estimation (KDE), which enables continuous estimation of the empirical distribution of the integrated risk, as shown in Figure 22.

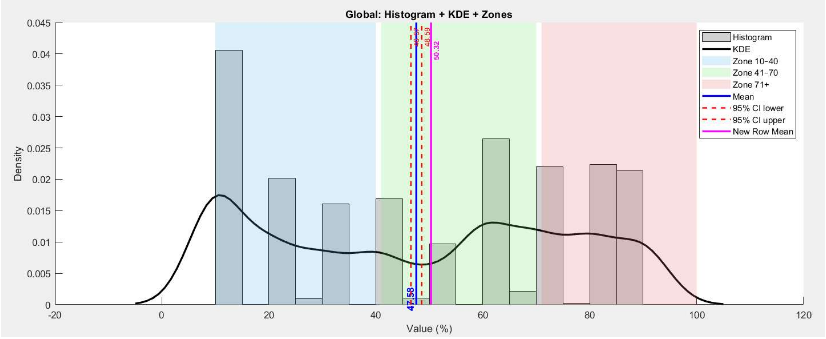

Figure 22. Empirical distribution of the integrated risk estimated using Kernel Density Estimation (KDE).

Figure 23 presents the distribution of the integrated risk for the element "driver", defined through 17 linguistic variables out of a total of 31 variables in the model. The obtained results show a clear concentration of values within the interval of 41–70%, with the maximum density occurring around a mean value of 55.48%. The calculated 95% confidence interval lies within the range of 54–58%, indicating a relatively stable distribution of risk associated with driver behavior in the analyzed sample.

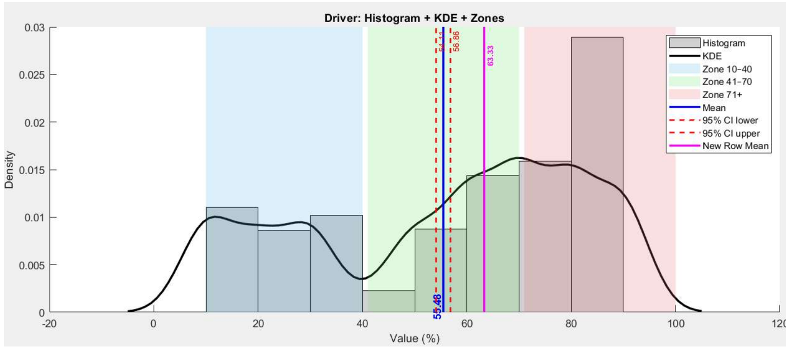

Figure 23. Empirical distribution of the integrated risk for the vector of linguistic variables for the element "driver", estimated using Kernel Density Estimation (KDE).

The fact that both the mean value and the confidence interval fall entirely within the range of 41–70% indicates that the analyzed cases are characterized by an elevated level of risk primarily determined by the human factor. This is most commonly manifested through inappropriate speed selection, delayed perception of the hazard, and inaccurate assessment of the moment of occurrence of the critical situation.

Within the framework of the analysis, an additional case was also examined, represented by a vector of linguistic variables, in which the risk assessment according to the proposed methodology is 61.65%, corresponding to the eighth risk level:

$$\begin{gathered}\Omega_4 = [10,20,80,10,30,10,10,40,80,70,10,60,40,40,90,\\ 10,40,10,90,30,80,90,90,80,60,50,30,80,70,80,70]\end{gathered} \quad (34)$$

The comparison of this value with the empirical distribution indicates that it lies in the upper part of the 41–70% interval and is significantly higher than the mean value of the sample, which suggests an increased influence of human-related factors.

The distribution of risk for the element "road–environment" is presented in Figure 24. The data show a concentration of values within the low-risk range, mainly between 10% and 40%, which is also confirmed by the shape of the KDE curve. The mean value is 35.50%, while the calculated 95% confidence interval lies within the range of 33.45–37.55%.

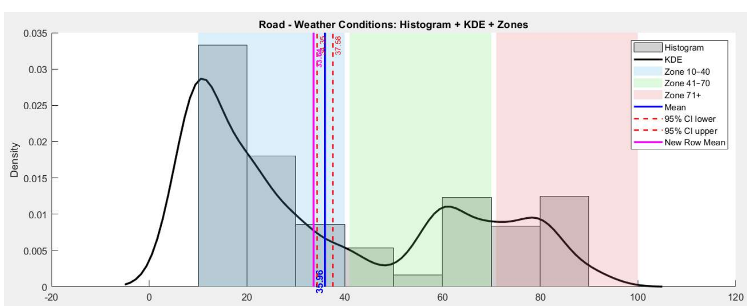

Figure 24. Empirical distribution of the integrated risk for the vector of linguistic variables corresponding to the element "road–environment", estimated using Kernel Density Estimation (KDE).

The value obtained for the analyzed case falls within this interval, indicating that the road and environmental conditions do not significantly deviate from the typical profile of the observed cases and therefore do not represent a dominant factor in accident occurrence.

Figure 25 presents the distribution of risk associated with the element "vehicle". The main concentration of values is observed within the range of 41–70%, with the mean value of the historical data approximately equal to 51.85%. The calculated 95% confidence interval is approximately 50–53%, indicating a stable distribution of risk associated with the technical characteristics of the vehicle.

Preprints.org (www.preprints.org) | NOT PEER-REVIEWED | Posted: 17 March 2026 doi:10.20944/preprints202603.1262.v1

The value obtained for the analyzed case falls within this interval and corresponds to the main maximum of the KDE curve, indicating that the technical condition of the vehicle and its contribution to the risk do not differ significantly from the typical observed values.

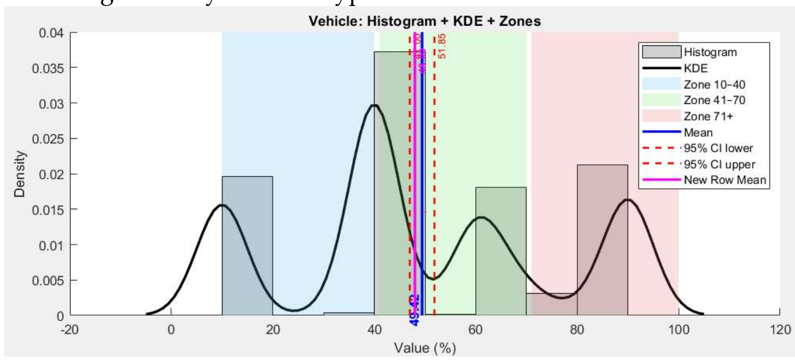

Figure 25. Empirical distribution of the integrated risk for the vector of linguistic variables corresponding to the element "vehicle", estimated using Kernel Density Estimation (KDE).

In summary, the results of the analysis, combined with the examination of more than 100 court decisions, indicate that driver behavior emerges as the primary factor in the formation of risk in pedestrian-involved road traffic accidents, while the influence of the road environment and the technical characteristics of the vehicle is considerably more limited. The proposed methodology, based on linguistic variables, dynamic modeling, and Kernel Density Estimation (KDE), demonstrates high applicability for quantitative risk assessment and enables the identification of critical zones with increased risk concentration. The analysis of empirical data and the results of dynamic simulations show that the integrated approach allows reliable identification of the key factors determining the level of risk, thereby providing a foundation for the development of intelligent systems for risk assessment and management in the transport system. The obtained results may serve as a basis for the development of driver assistance systems and intelligent transportation systems aimed at reducing the risk of pedestrian-involved accidents.

5. Conclusions

This study presents an integrated dynamic model for risk assessment and prevention of pedestrian-involved road traffic accidents. The model combines the analysis of real court cases, a system of linguistic variables, and mathematical modeling of the interaction between the vehicle and the pedestrian. Based on the analysis of 105 court decisions, 31 significant factors describing driver behavior, vehicle technical characteristics, and road-environmental conditions were identified and integrated into a unified model for quantitative risk assessment.

The obtained results show that even minimal delays in driver perception of a hazardous situation may lead to a significant increase in the risk of road traffic accidents. Numerical experiments conducted using the dynamic model demonstrate that a delay in driver reaction of approximately one second is sufficient to eliminate the technical possibility of avoiding a collision, regardless of the effectiveness of the braking system.

The results of the simulation studies confirm the critical importance of early hazard detection and highlight the need for implementing automated driver-assistance systems. It is demonstrated that automated control of the braking moment can substantially reduce reaction time and increase the probability of preventing a collision between a vehicle and a pedestrian.

The developed methodology and the proposed model can be applied both in engineering analyses of transport safety and in forensic investigations of road traffic accidents. The obtained results provide a basis for the development of intelligent systems for risk assessment and automated traffic management aimed at improving the safety of vulnerable road users within the transport system.

 doi:10.20944/preprints202603.1262.v1

The main scientific contribution of this study is the development of an integrated risk-assessment model that combines the analysis of real court cases, a system of linguistic variables, and dynamic modeling of vehicle–pedestrian interaction. The future research directions include the integration of machine learning algorithms for automated risk assessment and the improvement of the model by incorporating simulation-based experimental scenarios between road users, as well as its integration within intelligent transport systems and advanced driver-assistance systems.

Author Contributions: Conceptualization, H.U. and P.M.; methodology, H.U.; software, S.D.; data curation, V.U.; writing—original draft preparation, H.U.; writing—review and editing, H.U., P.M., V.U. and S.D. All authors have read and agreed to the published version of the manuscript.

Funding: Funding: The APC was funded by the Research and Development Sector of the Technical University of Sofia, Bulgaria.

Acknowledgments: This publication was developed within the project "Improvement of Research Capacity and Quality for International Recognition and Sustainability of the Technical University of Sofia", contract No. BG-RRP-2.004.0005. The authors acknowledge the support of the Research and Development Sector of the Technical University of Sofia.

Data Availability Statement: Not applicable.

Conflicts of Interest: The authors declare no conflict of interest.

References

1. Elvik, R. A Re-Parametrization of the Power Model of the Relationship between Speed and Road Safety. *Accident Analysis & Prevention* **2013**, *50*, 854–860. https://doi.org/10.1016/j.aap.2012.07.012
2. Billah, K.; Sharif, H.O.; Dessouky, S. Analysis of Pedestrian-Motor Vehicle Crashes in San Antonio, Texas. *Sustainability* **2021**, *13*, 6610. https://doi.org/10.3390/su13126610
3. Martinez-Ruiz, V.; Valenzuela-Martinez, M.; Lardelli-Claret, P.; Molina-Soberanes, D.; Moreno-Roldan, E.; Jimenez-Mejias, E. Factors Related to the Risk of Pedestrian Fatality after a Crash in Spain, 1993–2013. *Journal of Transport & Health* **2019**, *12*, 279–289. https://doi.org/10.1016/j.jth.2019.02.008
4. Kim, S.; Ulfarsson, G.F.; Shankar, V.N.; Mannering, F.L. Driver-Injury Severity in Single-Vehicle Crashes in California: A Mixed Logit Analysis of Heterogeneity in Vehicle Type and Driver Age. *Accident Analysis & Prevention* **2013**, *50*, 1073–1081. https://doi.org/10.1016/j.aap.2012.08.008
5. Febres, J.D.; Mariscal, M.A.; Herrera, S.; García-Herrero, S. Pedestrians' Injury Severity in Traffic Accidents in Spain: A Pedestrian Actions Approach. *Sustainability* **2021**, *13*, 6439. https://doi.org/10.3390/su13116439
6. Wang, K.; Zhang, W.; Jin, L.; Feng, Z.; Zhu, D.; Cong, H. Diagnostic Analysis of Environmental Factors Affecting the Severity of Traffic Crashes. *Traffic Injury Prevention* **2022**, *23*, 17–22. https://doi.org/10.1080/15389588.2021.1995602
7. Verstraete, T.; Muhammad, N. Pedestrian Collision Avoidance in Autonomous Vehicles: A Review. *Computers* **2024**, *13*, 78. https://doi.org/10.3390/computers13030078
8. Abdel-Aty, M.; Cai, Q.; Wu, Y.; Zheng, O. Evaluation of Automated Emergency Braking System's Avoidance of Pedestrian Crashes at Intersections under Occluded Conditions. *Accident Analysis & Prevention* **2022**, *174*, 106797. https://doi.org/10.1016/j.aap.2022.106797
9. Fu, X.; Wan, J.; Wu, D.; Jiang, W.; Ma, W.; Yang, T. Research on Vehicle AEB Control Strategy Based on Safety Time–Safety Distance Fusion Algorithm. *Mathematics* **2024**, *12*, 1905. https://doi.org/10.3390/math12121905
10. Cicchino, J.B. Effects of Automatic Emergency Braking Systems on Pedestrian Crash Risk. *Accident Analysis & Prevention* **2022**, *172*, 106686. https://doi.org/10.1016/j.aap.2022.106686
11. Jurecki, R.S.; Stańczyk, T.L. Driver Reaction Time to Lateral Entering Pedestrian in a Simulated Crash Traffic Situation. *Transportation Research Part F* **2014**, *27*, 27–36. https://doi.org/10.1016/j.trf.2014.08.006
12. Zhang, Y.; Li, Q.; Ma, X. Driver Reaction Time in Crash Avoidance Research: A Review of the Literature. *Transportation Research Part F* **2021**, *78*, 1–15. https://doi.org/10.1016/j.trf.2021.01.001

13. Li, Y.; Fan, W. Mixed Logit Approach to Modeling the Severity of Pedestrian Injury in Pedestrian-Vehicle Crashes. *Journal of Transportation Safety & Security* **2022**, *14*, 798–817. https://doi.org/10.1080/19439962.2020.1821850
14. Droździel, P.; Tarkowski, S.; Rybicka, I.; Wrona, R. Drivers' Reaction Time Research in Real Traffic Conditions. *Open Engineering* **2020**, *10*, 4–9. https://doi.org/10.1515/eng-2020-0004
15. Majerčák, Ľ.; Blišťan, P.; Kováčik, P.; Kováčik, M. A Driving Simulator Study among Professional-Truck Drivers. *Mathematics* **2022**, *10*, 1489. https://doi.org/10.3390/math10091489
16. Cicchino, J.B. Effectiveness of Forward Collision Warning and Autonomous Emergency Braking Systems. *Accident Analysis & Prevention* **2017**, *99*, 142–152. https://doi.org/10.1016/j.aap.2016.11.009
17. Cicchino, J.B. Effects of Forward Collision Warning and Automatic Emergency Braking on Rear-End Crashes in Pickup Trucks. *Accident Analysis & Prevention* **2017**, *99*, 142–152. https://doi.org/10.1016/j.aap.2016.11.009
18. Aleksa, M.; Schaub, A.; Erdelean, I.; et al. Impact Analysis of Advanced Driver Assistance Systems Regarding Road Safety. *European Transport Research Review* **2024**, *16*, 54. https://doi.org/10.1186/s12544-024-00654-0
19. A Systematic Review of Autonomous Emergency Braking System: Impact Factors, Key Technologies, and Effect Evaluation. *Journal of Advanced Transportation* **2022**, Article 1188089. https://doi.org/10.1155/2022/1188089
20. Evaluating Forward Collision Warning and Autonomous Emergency Braking Systems Using Dashboard Cameras. *SAE Technical Paper* **2024**. https://doi.org/10.4271/2024-26-0031
21. Lyubenov, D.; Kadirova, S.; Kadikyanov, G.; Kolev, Z.; Topchu, D. Experimental Determination of Bicycles and Electric Bicycle Stopping Distance. *Engineering Proceedings* **2024**, *7*, 26. https://doi.org/10.3390/engproc2024070026
22. Aghabayk, K.; Esmailpour, J.; Sarvi, M. Modeling Vehicle Overtaking Maneuvers on Two-Lane Rural Roads: A Driving Simulator Study. *Accident Analysis & Prevention* **2015**, *83*, 153–161. https://doi.org/10.1016/j.aap.2015.07.006
23. Abdel-Aty, M.; Lee, J.; Yu, R. Analysis of Pedestrian Crashes Using Machine Learning Algorithms. *Accident Analysis & Prevention* **2019**, *131*, 285–293. https://doi.org/10.1016/j.aap.2019.05.030
24. Uzunov, H.; Dimitrov, K.; Dechkova, S. Experimental Determination of the Tire-Road Friction Coefficient for a Vehicle with Anti-Lock Braking System. *AIP Conference Proceedings* **2021**. https://doi.org/10.1063/5.0103769
25. Andersen, M.H.; Wiben, R. *Design of Slip-Based Active Braking and Traction Control System for the Electric Vehicle QBEAK*; Master's Thesis, Aalborg University: Aalborg, Denmark. https://projekter.aau.dk/projekter/files/65240659/Design_of_Slip_based_Active_Braking_and_Traction_Control_Sytem_for_the_Electric_Vehicle_QBEAK.pdf
26. Basu, S.; Cicchino, J.B. Modeling the Effect of Time Pressure on Driver Reaction Time. *Accident Analysis & Prevention* **2020**, *142*, 105824. https://doi.org/10.1016/j.aap.2020.105824
27. Uzunov, H.; Dechkova, S.; Dimitrov, K. Mechanical Mathematical Modeling of a Car Accident Caused by Sudden Mechanical Failure. *Journal of Engineering Science and Technology Review* **2021**, *14*, 61–68. https://doi.org/10.25103/jestr.144.08
28. Uzunov, H.; Matzinski, P.; Dechkova, S.; Dimov, N. Systems Engineering Information Model of Vehicle-Pedestrian Collisions. *Cybernetics and Information Technologies* **2021**, *21*, 151–168. https://doi.org/10.2478/cait-2021-0011
29. Parzen, E. On Estimation of a Probability Density Function and Mode. *Annals of Mathematical Statistics* **1962**, *33*, 1065–1076. https://doi.org/10.1214/aoms/1177704472